Results

Retrovirus transduction of shRNA can protect from HCV replication

Retrovirus vectors propagated from pLNCshRNA-HCV and pLNCshRNA-Control were used to infect Huh7 cells, and cell lines were established that constitutively express shRNA-HCV and shRNA-Control (Huh7/shRNA-HCV and Huh7/shRNA-Control, respectively). There were no differences in the cell morphology or growth rate between shRNA-transduced and non-transduced Huh7 cells (data not shown). The HCV replicon, pRep-Fluc, was transfected into Huh7/shRNA-HCV, Huh7/shRNA-Control and naive Huh7 cells by electroporation. In Huh7/shRNA-Control and naive Huh7 cells, the initial luciferase activity at 4 h decreased temporarily, which represents decay of the transfected replicon RNA, but increased again at 48 h and 72 h, which demonstrate de novo synthesis of the HCV replicon RNA. In contrast, transfection into Huh7/shRNA-HCV cells resulted in a decrease in the initial luciferase activity, reaching background by 72 h (Fig. 3a). Similarly, transfection of the replicon, pRep-BSD, into Huh7 cells and BSD selection yielded numerous BSD-resistant colonies in the naive Huh7 (832 colonies) and Huh7/shRNA-Control cell lines (740 colonies), while transfection of Huh7/shRNA-HCV, which expressed shRNA-HCV, yielded obviously fewer colonies (five colonies), indicating reduction of colony forming units by ~10^2 (Fig. 3b). There was no difference in shape, growth or viability between cells expressing the shRNA or not. These results indicated that cells expressing HCV-directed shRNA following retrovirus transduction acquired resistance to HCV replication.

Effect of recombinant adenoviruses expressing shRNA on *in vitro* HCV replication

We investigated subsequently the effects of recombinant adenovirus vectors expressing shRNA. AxshRNA-HCV and AxshRNA-Control were used separately to infect Huh7/pRep-Feo cells, and the internal luciferase activities were measured sequentially (Fig. 4a). AxshRNA-HCV caused continuous suppression of HCV RNA replication. Six days postinfection, the luciferase activities fell to background levels. In contrast, the luciferase activities of the Huh7/pRep-Feo cells infected with AxshRNA-Control did not show any significant changes compared with untreated Huh7/pRep-Feo cells (Fig. 4a). The dimethylthiazol carboxymethoxyphenyl sulfophenyl tetrazolium (MTS) assay showed no significant difference between cells that were infected by recombinant adenovirus and uninfected cells (Fig. 4b). In the northern blotting analysis, the cells were harvested 6 days after infection with the adenovirus at an MOI of 1. Feo-replicon RNA of 9.6 kb, which was detectable in the untreated Huh7/pRep-Feo cells and in the cells infected with AxshRNA-Control, diminished substantially following infection with the AxshRNA-HCV (Fig. 4c). Densitometries showed that the intracellular levels of the replicon RNA in the Huh7/pRep-Feo cells correlated well with the internal luciferase activities. Similarly in the western blotting, cells were harvested 6 days after infection with adenovirus. Levels of the HCV NS4A and NS5A proteins that were translated from the HCV replicon decreased following infection with the AxshRNA-HCV

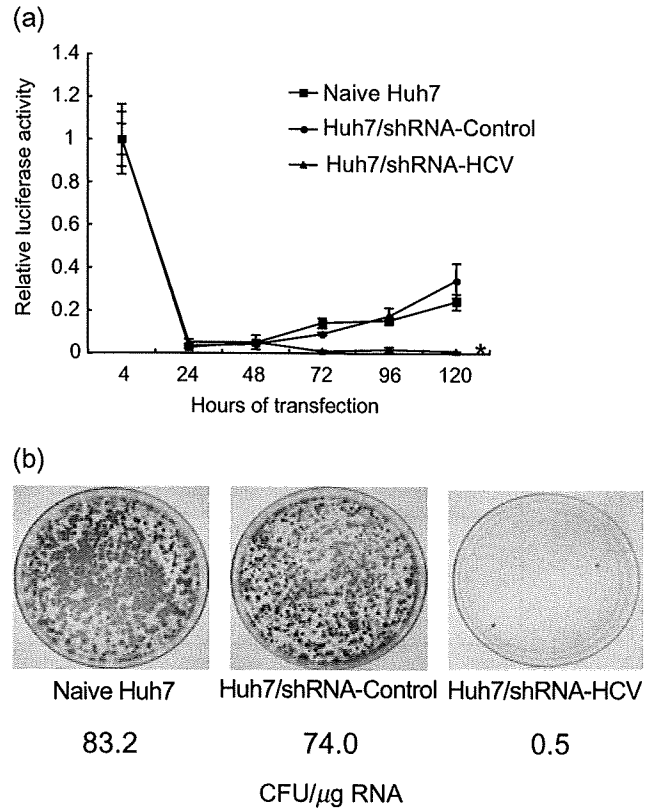

Figure 3 HCV replication can be inhibited by shRNA-HCV which was stably transfected into cells. Huh7/shRNA-HCV and Huh7/shRNA-Control stably express shRNA-HCV or shRNA-Control, respectively, following retroviral transduction. (a) Transient replication assay. An HCV replicon RNA, pRep-Fluc, was transfected into naive Huh7, Huh7/shRNA-HCV and Huh7/shRNA-Control cells. Luciferase activities of the cell lysates were measured serially at the times indicated, and the values were plotted as ratios relative to luciferase activities at 4 h. The luciferase activities at 4 h represent transfected replicon RNA. The data are mean ± SD. An asterisk denotes a *P*-value of less than 0.001 compared with the corresponding value of the naive Huh7 cells. (b) Stable colony formation assay. The HCV replicon, pRep-BSD, was transfected into naive Huh7, Huh7/shRNA-HCV and Huh7/shRNA-Control cells. The cells were cultured in the presence of blasticidin S (BSD) in the medium for ~3 weeks, and the BSD-resistant colonies were counted. These assays were repeated twice. The colony-forming units per microgram RNA (CFU/μg RNA) are shown at the bottom.

(Fig. 4d). These results indicated that the decrease in luciferase activities was due to specific suppressive effects of shRNA on expression of HCV genomic RNA and the viral proteins, and not due to non-specific effects caused by the delivery of shRNA or to toxicity of the adenovirus vectors.

Absence of interferon-stimulated gene responses by siRNA delivery

It has been reported that double-stranded RNA may induce interferon-stimulated gene (ISG) responses which cause instability of mRNA, translational suppression of proteins and apoptotic cell

Journal compilation © 2007 Journal of Gastroenterology and Hepatology Foundation and Blackwell Publishing Asia Pty Ltd

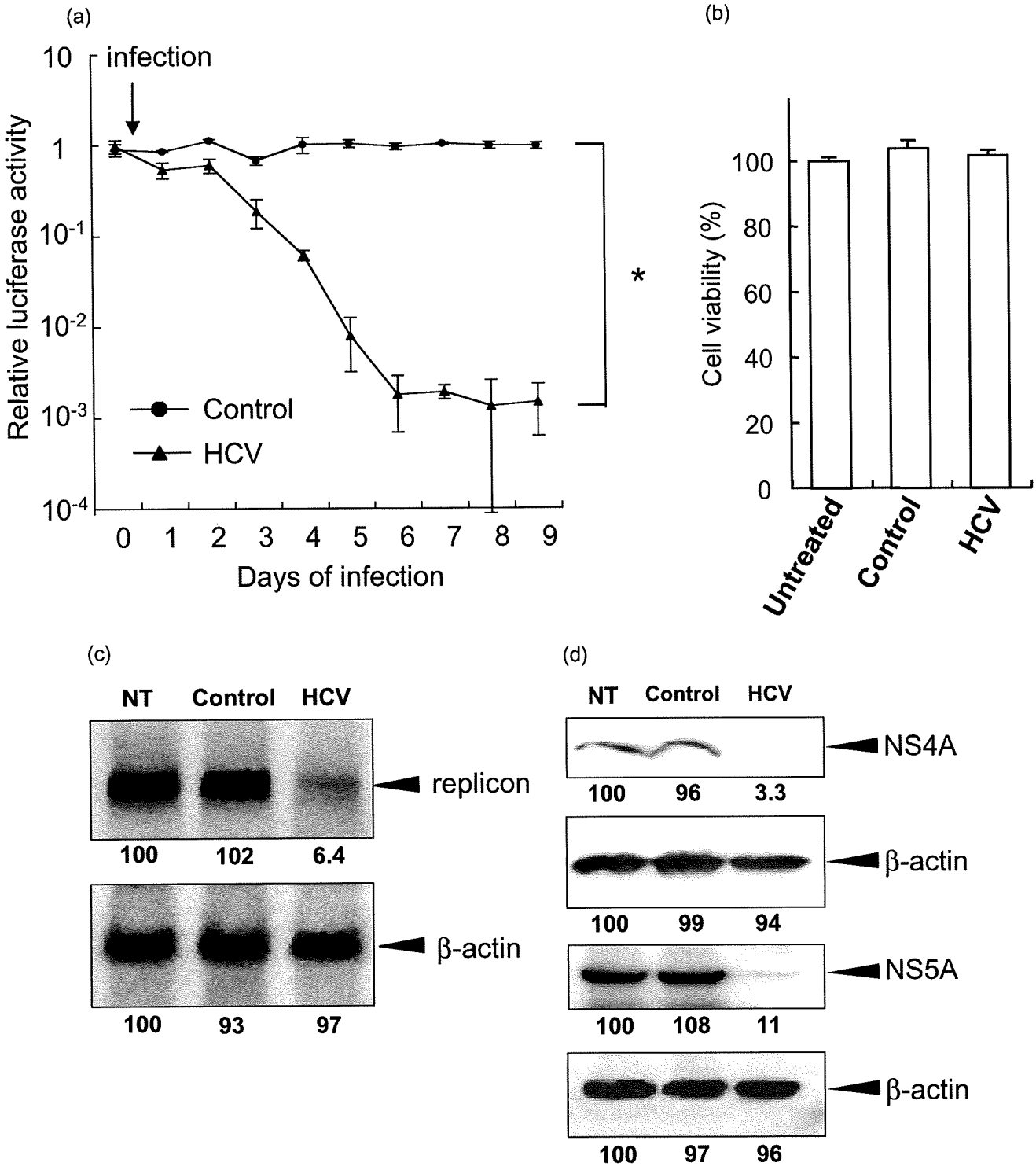

death.[18,30,31] Therefore, we examined the effects of the shRNA-expressing plasmids and adenoviruses on the activation of ISG expression in cells. The ISRE-reporter plasmid, pISRE-TA-Luc, and a control plasmid, peGFPneo, were transfected into Huh7 cells with plasmid pUC19-shRNA-HCV or pUC19-shRNA-Control, or adenovirus, AxshRNA-HCV or AxshRNA-Control, and the ISRE-mediated luciferase activities were measured. On day 2, the ISRE-luciferase activities did not significantly change in cells in which

Journal of Gastroenterology and Hepatology (2007) © 2007 The Authors
Journal compilation © 2007 Journal of Gastroenterology and Hepatology Foundation and Blackwell Publishing Asia Pty Ltd

Figure 4 Effect of a recombinant adenovirus expressing shRNA on HCV replicon. (a) Huh7/pRep-Feo cells were infected with AxshRNA-HCV or shRNA-Control at a multiplicity of infection (MOI) of 1. The cells were harvested, and internal luciferase activities were measured on day 0 though day 9 after adenovirus infection. Each assay was done in triplicate, and the value is displayed as a percentage of no treatment and as mean ± SD. An asterisk indicates a *P*-value of less than 0.05. (b) Dimethylthiazol carboxymethoxyphenyl sulfophenyl tetrazolium (MTS) assay of Huh7/pRep-Feo cells. Cells were infected with indicated recombinant adenoviruses at an MOI of 1. The assay was done at day 6 of infection. Error bars indicate mean + SD. (c) Northern blotting. The upper panel shows replicon RNA, and the lower panel shows beta-actin mRNA. (d) Western blotting. Total cell lysates were separated on NuPAGE gel, blotted and incubated with monoclonal anti-NS4A or anti-NS5A antibodies. The membrane was re-blotted with antibeta-actin antibodies. NT, untreated Huh7/pRep-Feo cells; Control, cells infected with AxshRNA-Control; HCV, cells treated with AxshRNA-HCV. In panels (b) and (c), cells were harvested on day 6 after adenovirus infection at an MOI of 1.

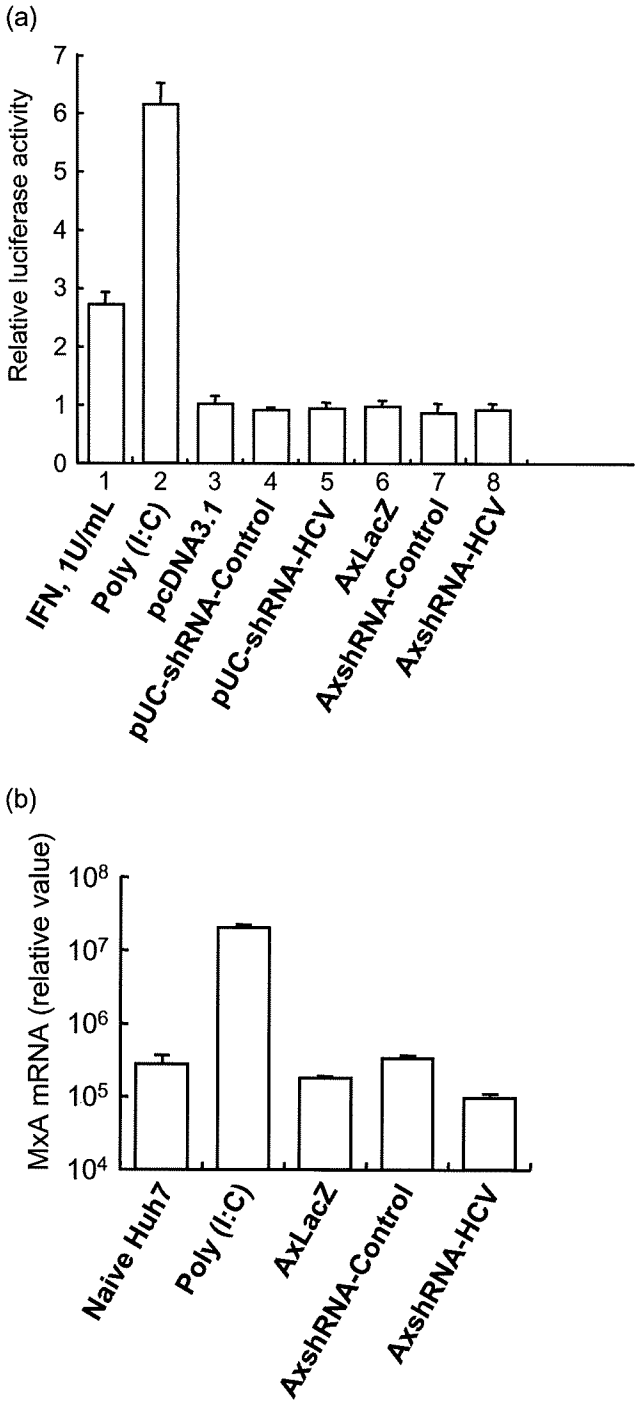

Figure 5 Interferon-stimulated gene responses by transfection of siRNA vectors. (a) Huh7 cells were seeded at 5×10^4 per well in 24-well plates on the day before transfection. As a positive control, 200 ng of pISRE-TA-Luc, or pTA-Luc, 1 ng of pRL-CMV, were transfected into a well using FuGENE-6 Transfection Reagent (Roche), and the cells were cultured with 1 U/mL of interferon (IFN) in the medium (lane 1). Lanes 3–5: 200 ng of pISRE-TA-Luc or pTA-Luc, and 1 ng of pRL-CMV were cotransfected with (lane2) 300 ng of poly (I : C), or 200 ng of plasmids (lane 3) pcDNA3.1, (lane 4) pUC19-shRNA-Control or (lane 5) pUC19-shRNA-HCV. Lanes 6–8: 200 ng of pISRE-TA-Luc or pTA-Luc, and 1 ng of pRL-CMV were transfected, and MOI = 1 of adenoviruses, (lane 6) AxLacZ, which expressed the beta-galactosidase (LacZ) gene under control of the chicken beta-actin (CAG) promoter as a control, (lane 7) AxshRNA-Control or (lane 8) AxshRNA-HCV were infected. Dual luciferase assays were performed at 48 h after transfection. The Fluc activity of each sample was normalized by the respective Rluc activity, and the respective pTA luciferase activity was subtracted from the pISRE luciferase activity. The experiment was done in triplicate, and the data are displayed as means + SD. (b) Huh7 cells were infected with indicated recombinant adenoviruses, AxLacZ, AxshRNA-Control and AxshRNA-HCV. RNA was extracted from each sample at day 6, and mRNA expression levels of an interferon-inducible MxA protein were quantified by the real-time RT-PCR analysis. Primers used were as follows: human MxA sense, 5′-CGA GGG AGA CAG GAC CAT CG-3′; human MxA antisense, 5′-TCT ATC AGG AAG AAC ATT TT-3′; human beta-actin sense, 5′-ACA ATG AAG ATC AAG ATC ATT GCT CCT CCT-3′; and human beta-actin antisense, 5′-TTT GCG GTG GAC GAT GGA GGG GCC GGA CTC-3′.

negative- or positive-control shRNA plasmids was transfected. (Fig. 5a). Similarly, the expression levels of an interferon-inducible MxA protein did not significantly change by transfection of shRNA-expression vectors (Fig. 5b). These results demonstrate that the shRNA used in the present study lack induction of the ISG responses both in the form of the expression plasmids and the adenovirus vectors.

Effect of siRNA and shRNA adenoviruses on HCV-JFH1 cell culture

The effects of HCV-targeted siRNA- and shRNA-expressing adenoviruses were confirmed by using HCV-JFH1 virus cell culture system. Transfection of the siRNA #331[14] into HCV-infected Huh7.5.1 cells resulted in substantial decrease of intracellular HCV RNA, while a control siRNA showed no effect (Fig. 6a). Similarly, infection of AxshRNA-HCV into Huh7.5.1/HCV-JFH1 cells specifically suppressed expression of HCV RNA (Fig. 6b).

Journal compilation © 2007 Journal of Gastroenterology and Hepatology Foundation and Blackwell Publishing Asia Pty Ltd

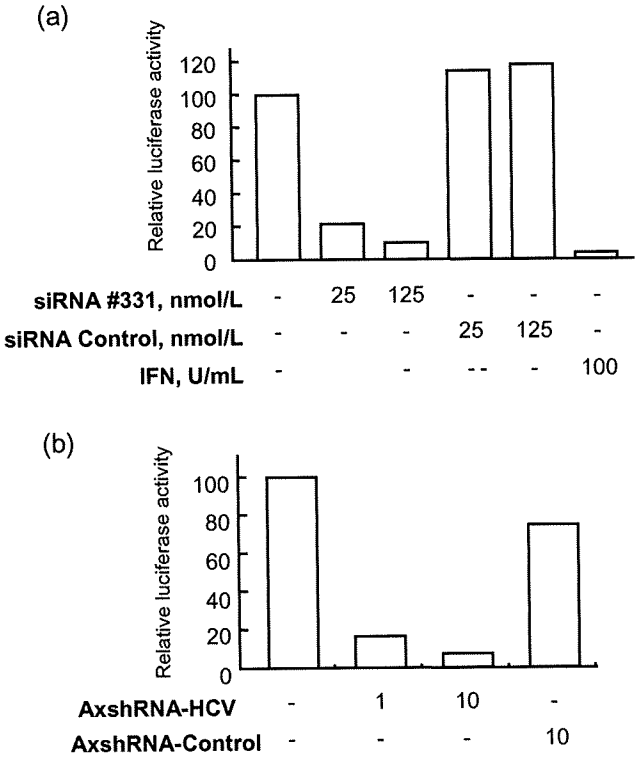

Figure 6 Effects of an siRNA and adenovirus expressing shRNA on HCV-JFH1 cell culture. (a) The siRNA #331, the siRNA-Control[14], (b) AxshRNA-HCV or AxshRNA-Control were, respectively, transfected or infected onto HV-JFH1-infected Huh7.5.1 cells. Seventy-two hours of the transfection or infection, expression level of HCV-RNA was quantified by real-time RT-PCR. The assays were repeated twice, and consistent results were obtained. IFN, recombinant interferon-alpha 2b.

Suppression of HCV-IRES-mediated translation *in vivo* by adenovirus expressing shRNA

The effects of the shRNA expression on the expression of the viral structural proteins *in vivo* were investigated using conditional HCV cDNA-transgenic mice, CN2-29.[28] Adenoviruses, AxshRNA-HCV, AxshRNA-Control or AxCAwl were injected into CN2-29 mice in combination with AxCANCre, an adenovirus expressing *Cre* DNA recombinase. The mice were killed on the fourth day after the injection, and the hepatic expression of the HCV core protein was measured. The expressed amounts of the core protein were 143.0 ± 56.2 pg/mg and 108.5 ± 42.4 pg/mg in AxCAwl and AxshRNA-Control-infected mice, respectively, and the expressed amount was significantly lower in mice injected with AxshRNA-HCV (28.7 ± 7.0 pg/mg, $P < 0.05$, Fig. 7a). Similarly, the induced expression of HCV core protein was not detectable by immunohistochemistry in AxshRNA-HCV infected liver tissue (Fig. 7c). Staining of a host cellular protein, albumin, was not obviously different between the liver infected with AxCAwl, AxshRNA-HCV and AxshRNA-Control (Fig. 7d). The expression levels of two ISG, IFN-beta and Mxl, in the liver tissue were not significantly different between individuals with and without injection of the adenovirus vectors (Fig. 7b). These results indicate specific shRNA silencing of HCV structural protein expression in the liver.

Discussion

The requirements to achieve a high efficiency using RNAi are: (i) selection of target sequences that are the most susceptible to RNAi; (ii) persistence of siRNA activity; and (iii) efficient *in vivo* delivery of siRNA to cells. We have used an shRNA sequence that was derived from a highly efficient siRNA (siRNA331), and constructed a DNA-based shRNA expression cassette that showed competitive effects with the synthetic siRNA (Fig. 2).[14] The shRNA-expression cassette does not only allow extended half-life of the RNAi, but also enables use of gene-delivery vectors, such as virus vectors. As shown in the results, a retrovirus vector expressing shRNA-HCV could stably transduce cells to express HCV-directed shRNA, and the cells acquired protection against HCV subgenomic replication (Fig. 3). An adenovirus vector expressing shRNA-HCV resulted in suppression of HCV subgenomic and protein expression by around three logs to almost background levels (Fig. 4). Consistent results were obtained by using an HCV cell culture (Fig. 6). More importantly, we have demonstrated *in-vivo* effects on viral protein expression in the liver using a conditional transgenic mouse model (Fig. 7). These results suggest that efficient delivery of siRNA could be effective against HCV infection *in vivo*.

An obstacle to applying siRNA technology to treat virus infections is that viruses are prone to mutate during their replication.[32] HCV continuously produces mutated viral strains to escape immune defense mechanisms. Even in a single patient, the circulating HCV population comprises a large number of closely related HCV sequence variants called quasispecies. Therefore, siRNA targeting the protein-coding sequence of the HCV genome, which have been reported by others,[15–19] may vary considerably among different HCV genotypes, and even among strains of the same genotype.[33] Our shRNA sequence targeted the 5′-UTR of HCV RNA, which is the most conserved region among various HCV isolates.[33] In addition, the structural constraints on the 5′-UTR, in terms of its requirement to direct internal ribosome entry and translation of viral proteins, might not permit the evolution of escape mutations. Our preliminary results have shown that the siRNA-HCV suppressed replication of an HCV genotype 2a replicon[34] to the same extent as the HCV 1b replicon.

Although the siRNA techniques rely on a high degree of specificity, several studies report siRNA-induced non-specific effect that may result from induction of ISG responses.[18,31] These effects may be mediated by activation of double-strand RNA-dependent protein kinase, toll-like receptor 3,[35] or possibly by a recently identified RNA helicase, RIG-I.[36] It remains to be determined whether these effects are generally induced by every siRNA construct. Sledz *et al.* have reported that transfection of two siRNA induced cellular interferon responses,[37] while Bridge *et al.* report that shRNA-expressing plasmids induced an interferon response but transfection of synthetic siRNA did not.[31] Speculatively, these effects on the interferon system might be construct dependent. Our shRNA-expression plasmids and adenoviruses did not activate ISG responses *in vitro* (Fig. 5a,b) or *in vivo* (Fig. 7b). We have preliminarily detected phosphorylated PKR (P-PKR) by western

Journal of Gastroenterology and Hepatology (2007) © 2007 The Authors
Journal compilation © 2007 Journal of Gastroenterology and Hepatology Foundation and Blackwell Publishing Asia Pty Ltd

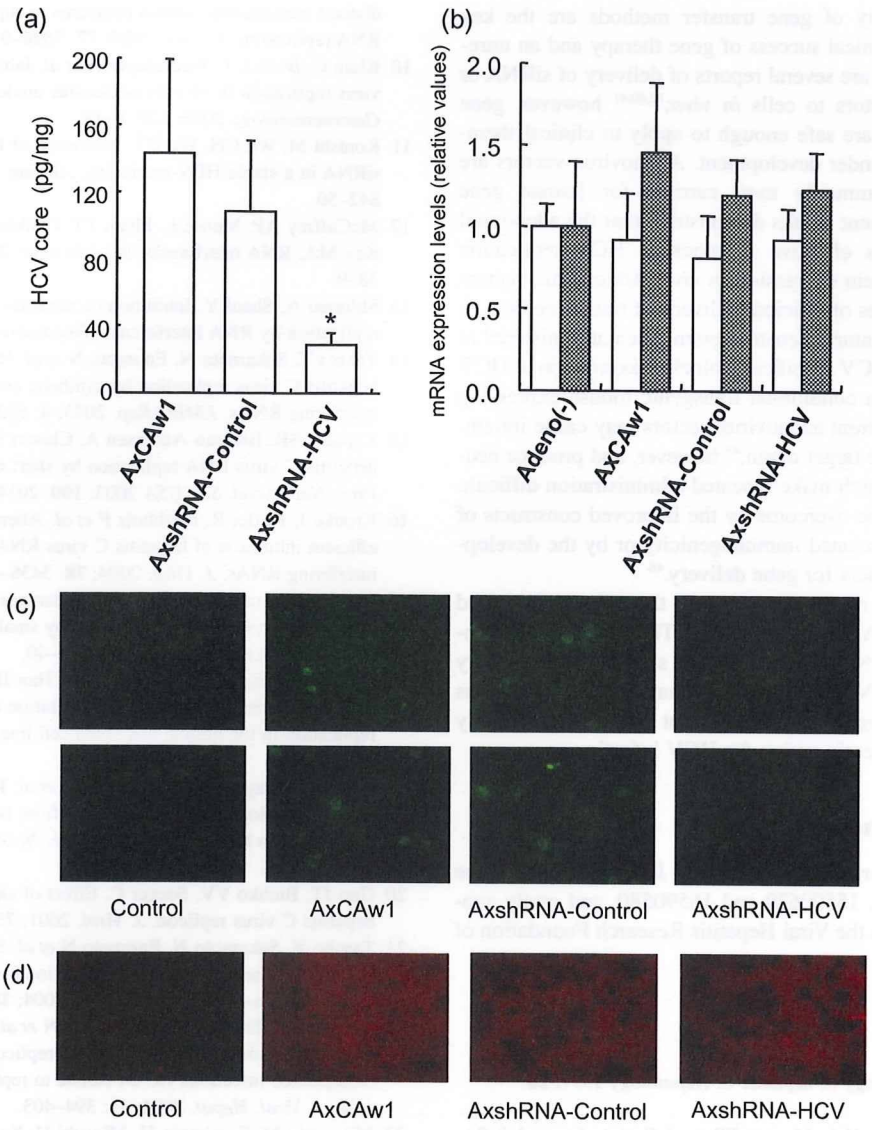

Figure 7 Effects of a recombinant adenovirus expressing shRNA on HCV core protein expression in CN2-29 transgenic mice. CN2-29 transgenic mice were administered with 1×10^9 PFU of AxCANCre combined with 6.7×10^8 PFU of AxshRNA-HCV, AxshRNA or AxCAw1. The mice were killed on day 4 after injection. (a) Quantification of HCV core protein in liver. Liver tissues were homogenized and used to determine the amount of HCV core protein. Each assay was done in triplicate, and the values are displayed as mean ± SD. Asterisk indicates *P*-value of less than 0.05. (b) Expression levels of mouse interferon-beta (white bars) and Mx1 (shaded bars) mRNA in the mouse liver tissue were quantified by the real-time RT-PCR analyses. Primers used were as follows: mouse interferon-beta sense, 5′-ACA GCC CTC TCC ATC AAC TA-3′; mouse interferon-beta antisense, 5′-CCC TCC AGT AAT AGC TCT TC-3′; mouse Mx1 sense, 5′-AGG AGT GGA GAG GCA AAG TC-3′; mouse Mx1 antisense, 5′-CAC ATT GCT GGG GAC TAC CA-3′; mouse beta-actin sense, 5′-ACT CCT ATG TGG GTG ACG AG-3′; mouse beta-actin antisense, 5′-ATA GCC CTC GTA GAT GGG CA-3′. Adeno (-) denotes mice without adenovirus administration. (c) Immunofluorescence microscopy of HCV core protein in the liver tissue. Liver sections of mice were stained using rabbit anticore polyclonal antibody and normal rabbit IgG as a negative control. The upper photographs were obtained at 400× magnification, and the lower photographs were at 1000×. (d) Immunofluorescence microscopy of albumin in liver. Liver sections from the mice were fixed and stained using rabbit antialbumin antibody and normal rabbit IgG as a negative control.

blotting, and found no apparent increase of P-PKR (data not shown). These results indicate that these target sequences and structures are of sufficient specificity to silence the target gene without eliciting non-specific interferon responses.

Beside the canonical action of siRNA, a sequence-specific cleavage of target mRNA, the siRNA could act as a micro-RNA that suppresses translational initiation of mRNA,[38] or it could mediate transcriptional gene silencing.[39] Regarding our *in-vivo* experiments, it was difficult to differentially analyze the effect of siRNA at individual sites of action because post-translational effect of siRNA concomitantly destabilizes target mRNA, which leads to apparent decrease of mRNA transcripts.

Efficiency and safety of gene transfer methods are the key determinants of the clinical success of gene therapy and an unresolved problem. There are several reports of delivery of siRNA or siRNA-expression vectors to cells *in vivo*;[12,40,41] however, gene delivery methods that are safe enough to apply to clinical therapeutics are currently under development. Adenovirus vectors are one of the most commonly used carriers for human gene therapies.[42–44] Our present results demonstrate that the adenoviral delivery of shRNA is effective in blocking HCV replication *in vitro* and virus protein expression *in vivo*. Adenovirus vectors have several advantages of efficient delivery of transgene both *in vitro* and *in vivo* and natural hepatotropism when administered *in vivo*. The AxshRNA-HCV specifically blocked expression of HCV structural proteins in a conditional transgenic mouse expressing those proteins. The current adenovirus vectors may cause inflammatory reactions in the target organ,[45] however, and produce neutralizing antibodies which make repeated administration difficult. These problems may be overcome by the improved constructs of virus vectors with attenuated immunogenicity or by the development of non-viral carriers for gene delivery.[46]

In conclusion, our results demonstrate the effectiveness and feasibility of the siRNA expression system. The efficiency of adenovirus expressing shRNA that target HCV suggests that delivery and expression of siRNA in hepatocytes may eliminate the virus and that this RNA-targeting approach might provide a potentially effective future therapeutic option for HCV infection.

Acknowledgments

This study was supported by grants from Japan Society for the Promotion of Science, 15590629 and 16590580, and partly supported by a grant from the Viral Hepatitis Research Foundation of Japan.

References

1 Alter MJ. Epidemiology of hepatitis C. *Hepatology* 1997; **26**: 62S–65S.
2 Hadziyannis SJ, Sette H Jr, Morgan TR *et al.* Peginterferon-alpha2a and ribavirin combination therapy in chronic hepatitis C: a randomized study of treatment duration and ribavirin dose. *Ann. Intern. Med.* 2004; **140**: 346–55.
3 Fire A, Xu S, Montgomery M, Kostas S, Driver S, Mello C. Potent and specific genetic interference by double-stranded RNA in Caenorhabditis elegans. *Nature* 1998; **19**: 806–11.
4 Elbashir SM, Harborth J, Lendeckel W, Yalcin A, Weber K, Tuschl T. Duplexes of 21-nucleotide RNAs mediate RNA interference in cultured mammalian cells. *Nature* 2001; **411**: 494–8.
5 Coburn GA, Cullen BR. Potent and specific inhibition of human immunodeficiency virus type 1 replication by RNA interference. *J. Virol.* 2002; **76**: 9225–31.
6 Jacque JM, Triques K, Stevenson M. Modulation of HIV-1 replication by RNA interference. *Nature* 2002; **418**: 435–8.
7 Gitlin L, Karelsky S, Andino R. Short interfering RNA confers intracellular antiviral immunity in human cells. *Nature* 2002; **418**: 430–4.
8 Ge Q, Filip L, Bai A, Nguyen T, Eisen HN, Chen J. Inhibition of influenza virus production in virus-infected mice by RNA interference. *Proc. Natl. Acad. Sci. USA* 2004; **101**: 8676–81.
9 Wang C, Pflugheber J, Sumpter R Jr *et al.* Alpha interferon induces distinct translational control programs to suppress hepatitis C virus RNA replication. *J. Virol.* 2003; **77**: 3898–912.
10 Klein C, Bock CT, Wedemeyer H *et al.* Inhibition of hepatitis B virus replication in vivo by nucleoside analogues and siRNA. *Gastroenterology* 2003; **125**: 9–18.
11 Konishi M, Wu CH, Wu GY. Inhibition of HBV replication by siRNA in a stable HBV-producing cell line. *Hepatology* 2003; **38**: 842–50.
12 McCaffrey AP, Meuse L, Pham TT, Conklin DS, Hannon GJ, Kay MA. RNA interference in adult mice. *Nature* 2002; **418**: 38–9.
13 Shlomai A, Shaul Y. Inhibition of hepatitis B virus expression and replication by RNA interference. *Hepatology* 2003; **37**: 764–70.
14 Yokota T, Sakamoto N, Enomoto N *et al.* Inhibition of intracellular hepatitis C virus replication by synthetic and vector-derived small interfering RNAs. *EMBO Rep.* 2003; **4**: 602–8.
15 Kapadia SB, Brideau-Andersen A, Chisari FV. Interference of hepatitis C virus RNA replication by short interfering RNAs. *Proc. Natl. Acad. Sci. USA* 2003; **100**: 2014–18.
16 Kronke J, Kittler R, Buchholz F *et al.* Alternative approaches for efficient inhibition of hepatitis C virus RNA replication by small interfering RNAs. *J. Virol.* 2004; **78**: 3436–46.
17 Randall G, Grakoui A, Rice CM. Clearance of replicating hepatitis C virus replicon RNAs in cell culture by small interfering RNAs. *Proc. Natl. Acad. Sci. USA* 2003; **100**: 235–40.
18 Seo MY, Abrignani S, Houghton M, Han JH. Letter to the editor: small interfering RNA-mediated inhibition of hepatitis C virus replication in the human hepatoma cell line Huh-7. *J. Virol.* 2003; **77**: 810–12.
19 Wilson JA, Jayasena S, Khvorova A *et al.* RNA interference blocks gene expression and RNA synthesis from hepatitis C replicons propagated in human liver cells. *Proc. Natl. Acad. Sci. USA* 2003; **100**: 2783–8.
20 Guo JT, Bichko VV, Seeger C. Effect of alpha interferon on the hepatitis C virus replicon. *J. Virol.* 2001; **75**: 8516–23.
21 Tanabe Y, Sakamoto N, Enomoto N *et al.* Synergistic inhibition of intracellular hepatitis C virus replication by combination of ribavirin and interferon-alpha. *J. Infect. Dis.* 2004; **189**: 1129–39.
22 Maekawa S, Enomoto N, Sakamoto N *et al.* Introduction of NS5A mutations enables subgenomic HCV-replicon derived from chimpanzee-infectious HC-J4 isolate to replicate efficiently in Huh-7 cells. *J. Viral. Hepat.* 2004; **11**: 394–403.
23 Miyagishi M, Sumimoto H, Miyoshi H, Kawakami Y, Taira K. Optimization of an siRNA-expression system with an improved hairpin and its significant suppressive effects in mammalian cells. *J. Gene Med.* 2004; **6**: 715–23.
24 Li Y, Yokota T, Matsumura R, Taira K, Mizusawa H. Sequence-dependent and independent inhibition specific for mutant ataxin-3 by small interfering RNA. *Ann. Neurol.* 2004; **56**: 124–9.
25 Kanazawa N, Kurosaki M, Sakamoto N *et al.* Regulation of hepatitis C virus replication by interferon regulatory factor-1. *J. Virol.* 2004; **78**: 9713–20.
26 Wakita T, Pietschmann T, Kato T *et al.* Production of infectious hepatitis C virus in tissue culture from a cloned viral genome. *Nat. Med.* 2005; **11**: 791–6.
27 Zhong J, Gastaminza P, Cheng G *et al.* Robust hepatitis C virus infection in vitro. *Proc. Natl. Acad. Sci. USA* 2005; **102**: 9294–9.
28 Wakita T, Taya C, Katsume A *et al.* Efficient conditional transgene expression in hepatitis C virus cDNA transgenic mice mediated by the Cre/loxP system. *J. Biol. Chem.* 1998; **273**: 9001–6.
29 Kashiwakuma T, Hasegawa A, Kajita T *et al.* Detection of hepatitis C virus specific core protein in serum of patients by a sensitive fluorescence enzyme immunoassay (FEIA). *J. Immunol. Methods* 1996; **28**: 79–89.

 © 2007 The Authors
Journal compilation © 2007 Journal of Gastroenterology and Hepatology Foundation and Blackwell Publishing Asia Pty Ltd

30 Baglioni C, Nilsen TW. Mechanisms of antiviral action of interferon. *Interferon* 1983; **5**: 23–42.
31 Bridge A, Pebernard S, Ducraux A, Nicoulaz A, Iggo R. Induction of an interferon response by RNAi vectors in mammalian cells. *Nat. Genet.* 2003; **34**: 263–4.
32 Carmichael GG. Silencing viruses with RNA. *Nature* 2002; **418**: 379–80.
33 Okamoto H, Okada S, Sugiyama Y *et al.* Nucleotide sequence of the genomic RNA of hepatitis C virus isolated from a human carrier: comparison with reported isolates for conserved and divergent regions. *J. Gen. Virol.* 1991; **72**: 2697–704.
34 Kato T, Date T, Miyamoto M *et al.* Efficient replication of the genotype 2a hepatitis C virus subgenomic replicon. *Gastroenterology* 2003; **125**: 1808–17.
35 Alexopoulou L, Holt AC, Medzhitov R, Flavell RA. Recognition of double-stranded RNA and activation of NF-kB by Toll-like receptor 3. *Nature* 2001; **413**: 732–8.
36 Yoneyama M, Kikuchi M, Natsukawa T *et al.* The RNA helicase RIG-I has an essential function in double-stranded RNA-induced innate antiviral responses. *Nat. Immunol.* 2004; **5**: 730–7.
37 Sledz C, Holko M, de Veer M, Silverman R, Williams, B. Activation of the interferon system by short-interfering RNAs. *Nat. Cell. Biol.* 2003; **5**: 834–9.
38 Doench JG, Petersen CP, Sharp PA. siRNAs can function as miRNAs. *Genes Dev.* 2003; **17**: 438–42.
39 Morris KV. siRNA-mediated transcriptional gene silencing: the potential mechanism and a possible role in the histone code. *Cell. Mol. Life Sci.* 2005; **62**: 3057–66.
40 Xia H, Mao Q, Paulson HL, Davidson BL. siRNA-mediated gene silencing in vitro and in vivo. *Nat. Biotechnol.* 2002; **20**: 1006–10.
41 Zender L, Hutker S, Liedtke C *et al.* Caspase 8 small interfering RNA prevents acute liver failure in mice. *Proc. Natl. Acad. Sci. USA* 2003; **100**: 7797–802.
42 Akli S, Caillaud C, Vigne E *et al.* Transfer of a foreign gene into the brain using adenovirus vectors. *Nat. Genet.* 1993; **3**: 224–8.
43 Bajocchi G, Feldman SH, Crystal RG, Mastrangeli A. Direct in vivo gene transfer to ependymal cells in the central nervous system using recombinant adenovirus vectors. *Nat. Genet.* 1993; **3**: 229–34.
44 Davidson BL, Allen ED, Kozarsky KF, Wilson JM, Roessler BJ. A model system for in vivo gene transfer into the central nervous system using an adenoviral vector. *Nat. Genet.* 1993; **3**: 219–23.
45 Yang Y, Wilson JM. Clearance of adenovirus-infected hepatocytes by MHC class I-restricted CD4+ CTLs in vivo. *J. Immunol.* 1995; **155**: 2564–70.
46 Fleury S, Driscoll R, Simeoni E *et al.* Helper-dependent adenovirus vectors devoid of all viral genes cause less myocardial inflammation compared with first-generation adenovirus vectors. *Basic Res. Cardiol.* 2004; **99**: 247–56.

Journal compilation © 2007 Journal of Gastroenterology and Hepatology Foundation and Blackwell Publishing Asia Pty Ltd

GASTROENTEROLOGY 2008;134:1396–1405

Potential Relevance of Cytoplasmic Viral Sensors and Related Regulators Involving Innate Immunity in Antiviral Response

YASUHIRO ASAHINA,* NAMIKI IZUMI,* ITSUKO HIRAYAMA,* TOMOHIRO TANAKA,* MITSUAKI SATO,*,‡ YUTAKA YASUI,* NOBUTOSHI KOMATSU,*,‡ NAOKI UMEDA,* TAKANORI HOSOKAWA,* KEN UEDA,* KAORU TSUCHIYA,* HIROYUKI NAKANISHI,* JUN ITAKURA,* MASAYUKI KUROSAKI,* NOBUYUKI ENOMOTO,‡ MEGUMI TASAKA,§ NAOYA SAKAMOTO,§ and SHOZO MIYAKE*

*Department of Gastroenterology and Hepatology, Musashino Red Cross Hospital, Tokyo; ‡First Department of Internal Medicine, Faculty of Medicine, University of Yamanashi, Yamanashi; and §Department of Gastroenterology and Hepatology, Tokyo Medical and Dental University, Tokyo, Japan

Background & Aims: **Clinical significance of molecules involving innate immunity in treatment response remains unclear. The aim is to elucidate the mechanisms underlying resistance to antiviral therapy and predictive usefulness of gene quantification in chronic hepatitis C (CH-C).** ***Methods:*** **We conducted a human study in 74 CH-C patients treated with pegylated interferon α-2b and ribavirin and 5 nonviral control patients. Expression of viral sensors, adaptor molecule, related ubiquitin E3-ligase, and modulators were quantified.** ***Results:*** **Hepatic RIG-I, MDA5, LGP2, ISG15, and USP18 in CH-C patients were up-regulated at 2- to 8-fold compared with non-hepatitis C virus patients with a relatively constitutive Cardif. Hepatic RIG-I, MDA5, and LGP2 were significantly up-regulated in nonvirologic responders (NVR) compared with transient (TR) or sustained virologic responders (SVR). Cardif and RNF125 were negatively correlated with RIG-I and significantly suppressed in NVR. Differences among clinical responses in RIG-I/Cardif and RIG-I/RNF125 ratios were conspicuous (NVR/TR/SVR = 1.3:0.6:0.4 and 2.3:1.3:0.8, respectively). Like viral sensors, ISG15 and USP18 were significantly up-regulated in NVR (4-fold and 2.3-fold, respectively). Multivariate and receiver operator characteristic analyses revealed higher RIG-I/Cardif ratio, ISG15, and USP18 predicted NVR. Lower Cardif in NVR was confirmed by its protein level in Western blot. Also, transcriptional responses in peripheral blood mononuclear cells to the therapy were rapid and strong except for Cardif in not only a positive (RIG-I, ISG15, and USP18) but also in a negative regulatory manner (RNF125).** ***Conclusions:*** **NVR may have adopted a different equilibrium in their innate immune response. High RIG-I/Cardif and RIG-I/RNF125 ratios and ISG15 and USP18 are useful in identifying NVR.**

Infection with hepatitis C virus (HCV) is a common cause of chronic hepatitis, which progresses to cirrhosis and hepatocellular carcinoma in many patients.[1] Although combination therapy with pegylated interferon (PEG-IFN) α and ribavirin is now established as the standard treatment for chronic HCV infection genotype 1b, the sustained virologic response rate in these patients is still around 50%.[2–4] Moreover, physicians have also found that 20% of patients are nonvirologic responders (NVR; those whose HCV-RNA does not become negative during 48 weeks of combination therapy).[5] Prediction of NVR status is of clinical importance because these patients have no chance of achieving a sustained virologic response even after prolonged combination therapy.[6] However, mechanisms involving resistance to PEG-IFN-α and ribavirin have not been fully elucidated, and it is difficult to predict treatment responses before initiation of PEG-IFN-α and ribavirin combination therapy.

In vitro studies have suggested that an innate immune response in viral infection is an essential part of the host antiviral defense system.[7] HCV evades the host immune response through a complex combination of processes that include signaling interference, effector modulation, and continual viral genetic variation.[8] We hypothesized that liver tissue would show a consistent difference between responders and nonresponders in expression levels of the gene involved in innate immunity and IFN signal transduction. These differences could be used to predict treatment outcomes.

The retinoic acid–inducible gene I (RIG-I), a cytoplasmic RNA helicase, and the related melanoma differentia-

Abbreviations used in this paper: CARD, Caspase-recruiting domain; Cardif, caspase-recruiting domain adaptor inducing IFN-β; G3PDH, glyceraldehyde-3-phosphate dehydrogenase; HCV, hepatitis C virus; IPS-1, IFN-β promoter stimulator I; ISG15, IFN-stimulated gene 15; PEG-IFN, pegylated interferon; MDA5, melanoma differentiation associated gene 5; MAVS, mitochondrial antiviral signaling protein; NVR, nonvirologic responders; PBMC, peripheral blood mononuclear cell; RIG-I, retinoic acid-inducible gene I; RNF125, ring-finger protein 125; ROC, receiver operator characteristic; SVR, sustained viral responder; TR, transient responder; UBP43, ubiquitin-specific protease 43; USP18, ubiquitin-specific protease 18; VISA, virus-induced signaling adaptor.

© 2008 by the AGA Institute
0016-5085/08/$34.00
doi:10.1053/j.gastro.2008.02.019

Table 1. Patient Characteristics at Baseline According to Final Virologic Response

	SVR n = 30	TR n = 24	NVR n = 20	*P* value
Age (*y*)	52 ± 13	60 ± 8.7	60 ± 10	.04[a]
Female % (M/F)	47% (16/14)	63% (9/15)	60% (8/12)	.5[b]
Naïve & Relapser[c]/Non-responder[c]	26/4	20/4	14/6	.3[b]
BMI	24.6 ± 3.0	24.9 ± 4.4	24.0 ± 2.1	.6[a]
ALT (*IU/L*)	75 ± 57	65 ± 35	68 ± 41	1.0[a]
Hemoglobin (*g/dL*)	14.3 ± 1.6	14.1 ± 1.1	14.5 ± 1.7	.6[a]
Platelet count ($\times 10^3/\mu L$)	182 ± 62	169 ± 48	140 ± 39	.04[a]
Liver histology				
A1/A2/A3	19/8/3	14/8/1	10/10/0	.3[b]
F1/F2/F3	14/9/7	11/7/5	7/5/8	.7[b]
Viral load ($\times 10^6$ *IU/mL*)	1.6 ± 1.2	1.8 ± 1.1	1.6 ± 1.1	.8[a]
Viral decline rate (log_{10}/day)				
First phase	2.1 ± 0.9	1.5 ± 0.6	0.7 ± 0.5	<.0001[a]
Second phase	0.05 ± 0.05	0.04 ± 0.02	0.006 ± 0.008	<.0001[a]

ALT, alanine aminotransferase; BMI, body mass index.
[a]*P* values were determined by Kruskal–Wallis test.
[b]*P* values were determined by chi-square test.
[c]Response to previous IFN treatment.

tion-associated gene 5 (MDA5) play essential roles in initiating the host antiviral response by detecting intracellular viral dsRNA.[9,10] Caspase-recruiting domain (CARD) adaptor inducing IFN-β (Cardif), also called IFN-β promoter stimulator 1 (IPS-1), mitochondrial antiviral signaling protein (MAVS), and virus-induced signaling adaptor (VISA), is an adaptor molecule. Cardif connects RIG-I sensing to downstream signaling, resulting in IFN-β gene activation.[11–14] On the other hand, RIG-I sensing has been shown to be negatively regulated in a dominant-negative manner by LGP2,[10,15] a helicase related to RIG-I and MDA5 lacking CARD. Interestingly, the ubiquitin ligase ring-finger protein 125 (RNF125) has been recently shown to conjugate ubiquitin to RIG-I, MDA5 as well as Cardif, which results in suppressing the functions of these proteins.[16] Furthermore, these molecules are conjugated (ISGylated) by IFN-stimulated gene 15 (ISG15), a ubiquitin-like protein,[17] and ISG15 is specifically removed from ISGylated protein by ubiquitin-specific protease 18 (USP18), also called ubiquitin-specific protease 43 (UBP43).[18,19] Moreover, the NS3/4A protease of HCV specifically cleaves Cardif as part of its immune evasion strategy.[11,20] Therefore, the RIG-I/Cardif system and its regulatory systems have essential key functions in the innate antiviral response (see Supplementary Figure 1 online at www.gastrojournal.org). However, the clinical significance of these innate immune systems, especially in relevance to the treatment response, is unclear because findings in this field have been mainly obtained by in vitro experiments using cell lines.

The aims of this study were to elucidate the mechanisms underlying resistance to antiviral therapy in the clinical setting and to determine whether quantification of transcripts of positive and negative cytoplasmic viral sensors and related regulatory molecules involving innate immune system is useful in predicting responses to PEG-IFN-α and ribavirin combination therapy.

Patients and Methods

Patients

Among patients with biopsy-proven chronic hepatitis C hospitalized at the Musashino Red Cross Hospital, 74 patients of HCV genotype 1b with a high viral load (>100,000 IU/mL by Amplicor-HCV Monitor Assay; Roche Molecular Diagnostics Co, Tokyo, Japan) were included in the present study (Table 1). Patients with cirrhosis, autoimmune hepatitis, or alcoholic liver injury were excluded. No patient was positive for hepatitis B virus–associated antigen/antibody or anti–human immunodeficiency virus antibody. No patient received immunomodulatory therapy prior to the enrollment. Written informed consent was obtained from all the patients, and this study was approved by the Ethical Committee of Musashino Red Cross Hospital in accordance with the Helsinki Declaration. Five patients with nonviral liver disease (2 had autoimmune hepatitis and 3 had primary biliary cirrhosis) were included in the present study as controls.

Treatment Protocol

The patients were treated for 48 weeks with subcutaneous injections of PEG-IFN-α-2b (PegIntron; Schering-Plough Corporation, Kenilworth, NJ) at a dose of 1.5 $\mu g \cdot kg^{-1} \cdot week^{-1}$. Ribavirin (Rebetol; Schering-Plough Corporation) was administered concomitantly over the 48-week period, given orally twice daily at a total daily dose of 600 mg for the patients who weighed less than 60 kg and 800 mg for the patients who weighed between 60 and 80 kg. The dose of PEG-IFN-α-2b was reduced to 0.75 $\mu g \cdot kg^{-1} \cdot week^{-1}$ when either the neutrophil count was $<750/mm^3$ or the platelet count was $<80 \times 10^3/mm^3$. The dose of ribavirin was reduced to 600 mg/day when the hemoglobin concentration decreased to <10 g/dL.

Measurement of Gene Expression in the Liver

Liver biopsy was performed immediately before starting the therapy. After extraction of total RNA from liver biopsy specimens, the messenger RNA (mRNA) expression of positive and negative cytoplasmic viral sensors (RIG-I, MDA5, and LGP2), the adaptor molecule (Cardif), related ubiquitin E3-ligase (RNF125), and the modulators of these molecules (ISG15 and USP18) was quantified by real-time quantitative polymerase chain reaction (PCR) using primers specific for target genes. In brief, total RNA was extracted by the acid-guanidinium-phenol-chloroform method using Isogen (Nippon Gene Co Ltd, Toyama, Japan) from the liver biopsy specimen, which was 0.2–0.4 cm in length and 13 gauge in diameter. Complementary DNA (cDNA) was transcribed from 2 μg total RNA template in a 140-μL reaction mixture using a SYBR RT-PCR Kit (Takara Bio Co Ltd, Otsu, Japan) with random hexamer. Real-time quantitative PCR was performed using Smart Cycler version II (Takara Bio Co Ltd) with the SYBR RT-PCR Kit (Takara Bio Co Ltd) according to the manufacturer's instructions, and intercalating SYBR Green I (Molecular Probes Inc, Eugene, Oregon) was detected. Assays were performed in duplicate, and the expression levels of target genes were normalized to expression of the glyceraldehyde-3-phosphate dehydrogenase (G3PDH) gene and hydroxymethylbilane synthase, which is stable in the liver, as quantified using real-time quantitative PCR as internal controls. For accurate normalization, a set of 2 housekeeping genes was used in the present study. Sequences of primer sets were as follows: RIG-I: 5′-AAAGCATGCATGGTGTTCCAGA-3′, 5′-TCATTCGTGCATGCTCACTGATAA-3′; MDA5: 5′-ACATAACAGCAACATGGGCAGTG-3′, 5′-TTTGGTAAGGCCTGAGCTGGAG-3′; LGP2: 5′-ACAGCCTTGCAAACAGTACAACCTC-3′, 5′-GTCCCAAATTTCCGGCTCAAC-3′; Cardif: 5′-GGTGCCATCCAAAGTGCCTACTA-3′, 5′-CAGCACGCCAGGCTTACTCA-3′; RNF125: 5′-AGGGCACATATTCGGACTTGTCA-3′, 5′-CGGGTATTAAACGGCAAAGTGG-3′; ISG15: 5′-AGCGAACTCATCTTTGCCAGTACA-3′, 5′-CAGCTCTGACACCGACATGGA-3′; USP18: 5′-TGGTTCTGCTTCAATGACTCCAATA-3′, 5′-TTTGGGCATTTCCATTAGCACTC-3′; GAPDH: 5′-GCACCGTCAAGGCTGAGAAC-3′, 5′-TGGTGGTGAAGACGCCAGT-3′. hydroxymethylbilane synthase: 5′-AAGCGGAGCCATGTCTGGTAAC-3′, 5′-GTACCCACGCGAATCACTCTCA-3′.

Sequential Measurement of Gene Expression in Peripheral Blood Mononuclear Cells Before and During Therapy

To understand transcriptional response of the genes to PEG-IFN-α-2b and ribavirin therapy, serial expression of RIG-I, RNF125, Cardif, ISG15, and USP18 were determined before and during treatment in peripheral blood mononuclear cells (PBMC) in 14 patients (7 were sustained viral responders [SVR] and 7 were NVR). PBMC was obtained from whole blood samples collected before and at 4, 8, 24, 48, and 168 hours after the initiation of PEG-IFN-α-2b and ribavirin combination therapy. After extraction of total RNA from the PBMC, the expression of mRNA was quantified at each specified time point using real-time quantitative PCR as described above. Gene expression levels at each time point during treatment were calculated relative to baseline expression levels measured prior to IFN treatment.

Western Blotting

Western blotting was carried out in 9 patients (5 were SVR and 4 were NVR) and 3 non-HCV control subjects as described previously.[21] Liver biopsy specimen of ~10 mg was homogenized in 100 μL Complete Lysis-M (Roche Applied Science, Penzberg, Germany). Twenty micrograms of the homogenates were separated by SDS-PAGE and blotted onto a polyvinylidene difluoride Western blotting membrane. The membrane was incubated with the primary antibodies followed by a peroxidase-labeled anti-IgG antibody and visualized by chemiluminescence using the ECL Western blotting Analysis System (Amersham Biosciences, Buckinghamshire, United Kingdom). The anti-VISA mouse monoclonal antibody (BioDesign, Saco, ME) and anti-β-actin antibody (Sigma Chemical Co, St. Louis, MO) were used.

HCV Dynamics in Serum

To analyze the viral dynamics, HCV RNA was quantified just before and at 4, 8, and 24 hours and 2, 7, 14, 28, 56, and 84 days after the initiation of PEG-IFN-α-2b and ribavirin combination therapy, using real-time detection PCR, as reported previously.[22] For each patient, the viral decline curve was plotted on a semilogarithmic scale, and the slopes of the exponential viral declines were calculated for each viral decline phase with a straight-line fit of the data.

Definitions of Response to Therapy

A patient negative for serum HCV RNA during the first 6 months after the completion of PEG-IFN-α-2b and ribavirin combination therapy was defined as an SVR, and a patient for whom HCV RNA became negative at the end of therapy and reappeared after completion of therapy was defined as a transient responder (TR). A patient who was positive for HCV RNA even during the course of therapy was defined as an NVR. HCV RNA was determined with the Amplicor qualitative assay (Roche Molecular Diagnostics Co, Tokyo, Japan). The detection sensitivity of this assay is approximately 50 IU/mL.

Statistical Analysis

Categorical data were compared by the χ^2 test and Fisher exact test. Distributions of continuous variables were analyzed by Mann–Whitney U test for 2 groups. Kruskal–Wallis test was used for multiple group comparisons. All tests of significance were 2-tailed, and P values $< .05$ were considered statistically significant.

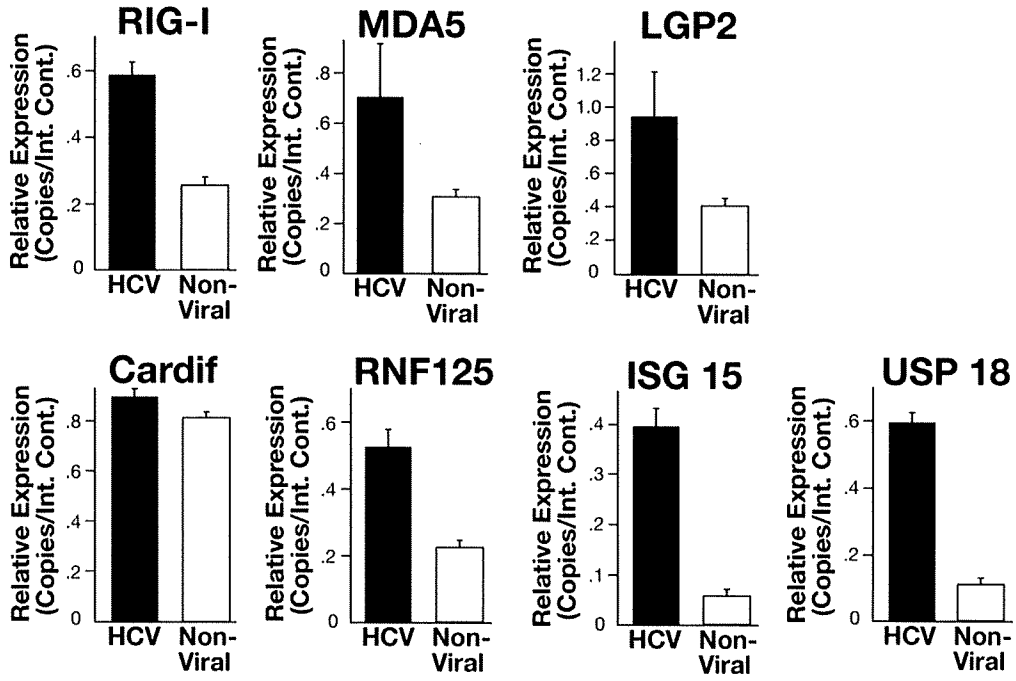

Figure 1. Comparison of hepatic gene expression levels between chronic hepatitis C patients (n = 74) and nonviral liver disease patients (n = 5). Expression levels of RIG-I, MDA5, LGP2, Cardif, RNF125, ISG15, and USP18 are shown. *Error bars* indicate the standard error. Upon HCV infection, expression of these genes except Cardif was stimulated. The *P* values determined by Mann–Whitney *U* test between 2 groups were as follows: RIG-I, *P* .02; MDA5, *P* .01; LGP2, *P* .005; Cardif, *P* .7; RNF125, *P* .06; ISG15, *P* .007; USP18, *P* .004.

Results

Patient Characteristics

According to the final virologic response, patients were classified into 3 groups: 30 were SVR, 24 were TR, and the remaining 20 were NVR, as shown in Table 1. Viral decline rates in NVR were significantly lower in both the first and second phases of HCV dynamics. It should be noted that most NVR patients exhibited no second-phase viral decline.

Data on factors that were available before starting the treatment were compared according to virologic response by univariate analysis. As shown in Table 1, only age and platelet count were associated with viral response, and no other clinical factors were predictive of NVR before initiation of the therapy.

Gene Expression Involving Innate Immunity in the Liver

First, we compared basal hepatic gene expression between the chronic hepatitis C patients (n = 74) and the nonviral liver disease patients (n = 5). As shown in Figure 1, levels of RIG-I, MDA5, LGP2, ISG15, and USP18 expression were significantly higher in the chronic hepatitis C patients than in the nonviral liver disease patients. However, there was no significant difference in levels of Cardif expression between the chronic hepatitis C and nonviral-related liver disease patients.

Next, to assess the relationship between baseline hepatic gene expression and treatment efficacy, levels of gene expression were compared based on the final virologic response. As shown in Figure 2, the hepatic expression levels of RIG-I, MDA5, and LGP2 were significantly higher in NVR than in SVR and TR. In marked contrast, hepatic Cardif expression was significantly lower in the NVR group. The hepatic expression of RNF125, which is specific E3-ubiquitin ligase for RIG-I, MDA5, and Cardif, was also significantly lower in the NVR group. Because negative correlation was found between RIG-I and Cardif or RNF125 expression, we calculated the ratio of RIG-I to Cardif or RNF125 expression levels. As shown in Figure 2, the difference among the groups was conspicuous when comparison was made with the RIG-I/Cardif ratio or RIG-I/RNF125 ratio. Moreover, the RIG-I/Cardif expression ratio before treatment was negatively and significantly correlated with the exponential viral decline rate in both the first and the second phases of HCV dynamics (first phase, $r = -0.4$, $P < .0005$; second phase, $r = -0.5$, $P < .0001$). Similar correlation was found between RIG-I/RNF125 ratio and viral decline rate (first phase, $r = -0.4$, $P = .004$; second phase, $r = -0.2$, $P = .09$, data not shown).

Like RIG-I and MDA5, intrahepatic expression levels of ISG15 and USP18 were significantly higher in NVR than in SVR and TR (Figure 2). When we assessed the correlation of these 2 genes in individual patients, we found a strong and significant correlation between ISG15 and USP18 ($r^2 = 0.88$, $P < .0001$). Levels of ISG15 and USP18 expression before treatment were negatively correlated with the exponential viral decline rates calculated from

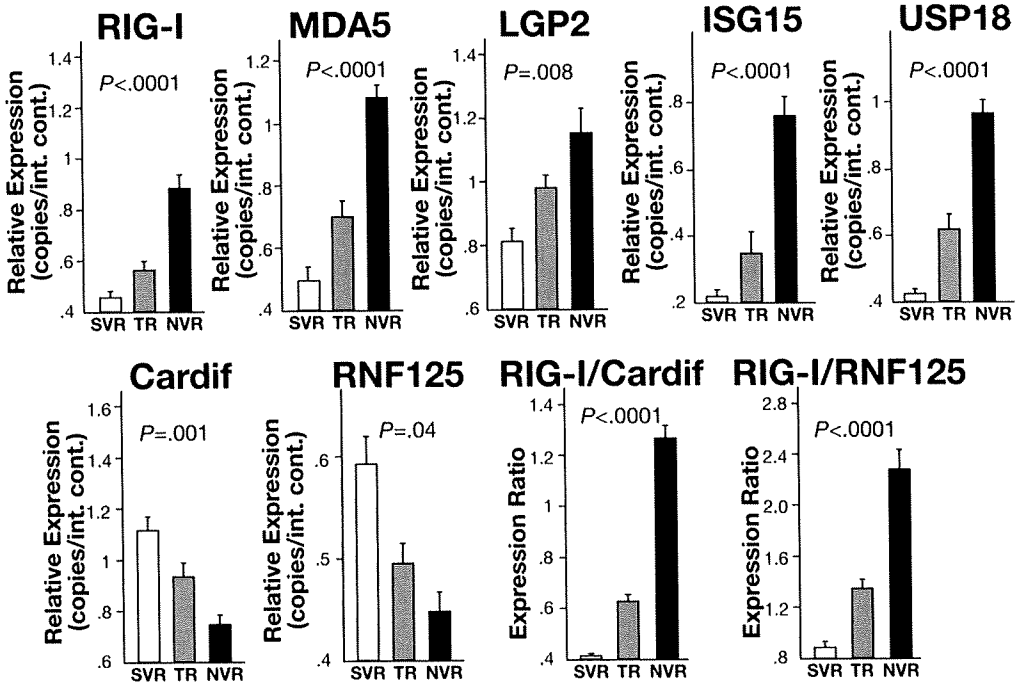

Figure 2. Comparison of hepatic gene expression levels according to final virologic outcome. Expression levels of RIG-I, MDA5, LGP2, ISG15, USP18, Cardif, RNF125, RIG-I/Cardif ratio, and RIG-I/RNF125 ratio are shown. *Open columns* indicate SVR (n = 30), *shaded columns* indicate TR (n = 24), and *solid columns* indicate NVR (n = 20). *Error bars* indicate the standard error. The *P* values were analyzed by the Kruskal–Wallis test.

the first and the second phases of HCV dynamics (ISG15, first phase, $r = -0.5$, $P < .0001$; ISG15, second phase, $r = -0.3$, $P = .02$; USP18, first phase, $r = -0.5$, $P < .0001$; USP18, second phase, $r = -0.3$, $P = .01$).

Receiver Operator Characteristic Analysis

To determine the usefulness of these gene quantifications as predictors, receiver operator characteristic (ROC) analysis was conducted (Figure 3). The area under the ROC curve for the RIG-I/Cardif ratio, ISG15, and USP18 was 0.91, 0.90, and 0.91, respectively, suggesting that quantification of these gene transcripts is of use for the prediction of NVR (Table 2). In addition, this analysis also suggested that RIG-I/Cardif ratio would be more specific for prediction of NVR, whereas ISG15 and USP18 would be more sensitive (Table 2).

Multivariate Analysis

Multivariate analysis for factors that were available before initiating therapy indicated that a higher ratio of RIG-I/Cardif and higher expression of ISG15 were independent factors that were associated with NVR (Table 3). In this analysis, USP18 was excluded because of its strong correlation with ISG15.

Protein Levels of Cardif in the Liver

Because hepatic expression of Cardif mRNA was significantly lower in NVR patients than in SVR patients,

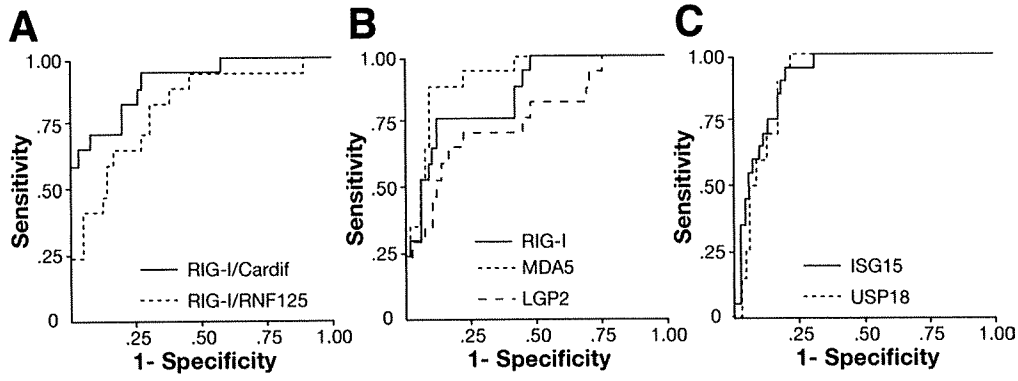

Figure 3. Receiver operator characteristic (ROC) curve for prediction of nonvirologic response. ROC curves were generated to compare (*A*) RIG-I/Cardif ratio (*solid line*) and RIG-I/RNF125 ratio (*shaded line*); (*B*) RIG-I (*solid line*), MDA5 (*shaded line*), and LGP2 (*dotted line*); and (*C*) ISG15 (*solid line*) and USP18 (*shaded line*).

Table 2. Area Under the ROC Curves, Sensitivity, Specificity, and Negative and Positive Predictive Values of Non-Virologic Responses

Variables	Az	95% CI	Cut-off	Sensitivity	Specificity	NPV[a]	PPV[b]
RIG-I	0.89	0.78–0.95	0.68	0.80	0.87	0.92	0.70
MDA5	0.92	0.86–0.98	0.84	0.82	0.89	0.93	0.74
LGP2	0.76	0.63–0.90	1.03	0.65	0.72	0.85	0.46
RIG-I/Cardif	0.91	0.84–0.99	0.88	0.75	0.91	0.91	0.75
RIG-I/RNF125	0.81	0.69–0.93	1.05	0.82	0.62	0.91	0.43
ISG15	0.91	0.85–0.97	0.36	0.90	0.81	0.96	0.64
USP18	0.90	0.84–0.96	0.67	0.90	0.83	0.96	0.67

[a]NPV, negative predictive value.
[b]PPV, positive predictive value.

we determined the basal protein expression levels of Cardif in the liver in NVR and SVR patients. Western blot analysis demonstrated a single Cardif product in all samples (Figure 4*A*). Similar to Cardif mRNA expression, mean Cardif expression in NVR patients was significantly lower than that in SVR (Figure 4*B*, $P = .01$). The cleavage product of Cardif, which has been reported by Loo et al,[23] was not detected in our analyses.

Transcriptional Responses to PEG-IFN-α-2b and Ribavirin Therapy in PBMC

Sequential analysis in response to PEG-IFN-α-2b and ribavirin demonstrated a rapid and strong induction of RIG-I, ISG15, and USP18 mRNA expression, which peaked 8 hours after PEG-IFN-α-2b administration (Figure 5). A greater fold change of these peak inductions was observed in SVR patients compared with NVR patients, although statistical significance was not achieved. In marked contrast, RNF125 expression profile in response to PEG-IFN-α-2b was triphasic, and consisted of (1) rapid and strong suppression peaked at 8 hours after administration, (2) increased 1.5- to 2-fold above baseline level during 24–48 hours after the administration, and (3) gradually decreased to baseline level (Figure 5). The rapid suppression and subsequent increase following PEG-IFN-α-2b administration tended to have a greater fold change in NVR patients compared with those in SVR patients. In contrast from RIG-I, ISG15, USP18, and RNF125, Cardif expression profile was relatively constitutive, and transcriptional response to PEG-IFN was weak (Figure 5).

Discussion

In the present study, we found that baseline expression levels of intrahepatic viral sensors and related regulatory molecules were significantly associated with the final virologic outcome in patients with chronic hepatitis C who were treated with PEG-IFN-α-2b and ribavirin combination therapy: up-regulation of RIG-I, MDA5, LGP2, ISG15, and USP18 and lower expression of Cardif and RNF125 could predict nonresponse to subsequent treatment with PEG-IFN-α-2b and ribavirin. The positive predictive value of a high ratio of expression of RIG-I to Cardif (>0.88) for NVR was the highest at a value of 0.75, and the negative predictive values of high expression of ISG15 (>0.36/internal control) and USP18 (>0.67/internal control) were the highest at values of both 0.96. These data may be of use in predicting clinical responses to the PEG-IFN-α and ribavirin combination before initiating therapy.

Table 3. Multivariate Analysis for the Factors Associated With Non-Virologic Response

Variable	Odds ratio	95% CI	*P* value
RIG-I/Cardif Ratio (by 0.1)	1.5	1.1–2.1	.008
RIG-I/RNF125 Ratio (by 0.1)	1.2	1.0–2.5	.1
ISG15 (by 0.1/internal control)	1.5	1.1–2.0	.01
Age (by 1 y)	1.0	0.9–1.1	.6
Platelet count (by $1 \times 10^4/\mu L$)	1.2	0.9–1.5	.07

Previously, large randomized controlled trials identified several pretreatment factors associated with the final virologic outcome, such as genotype, HCV RNA level, degree of fibrosis, age, body weight, ethnicity, and steatosis.[24] However, these findings lead us to believe that predicting the final virologic response before initiating PEG-IFN-α and ribavirin is difficult. Indeed, only age and platelet count were associated with the outcome in our patients with genotype 1b and a high viral load. Currently, the final response can be gauged only after treatment has been initiated. Although an early viral response at 12 weeks suggests the eventual outcome with 60%–90% accuracy,[25] a 12-week regimen is associated with adverse effects and is expensive. Therefore, this study investigated the baseline expression of genes involving innate immunity that may have significant effects on clinical outcomes.

In the present study, we demonstrated that RIG-I and MDA5 were inducible upon HCV infection and that expression of these intrahepatic positive viral sensors was up-regulated in NVR. In vitro studies have suggested that RIG-I and MDA5 play a pivotal role in the regulation of IFN production and augment the production of IFN via an amplification circuit. These results suggest that expression of RIG-I and MDA5 and related amplification system may be up-regulated by endogenous IFN at a higher baseline level in NVR patients. However, HCV elimination by subsequent exogenous IFN is insufficient

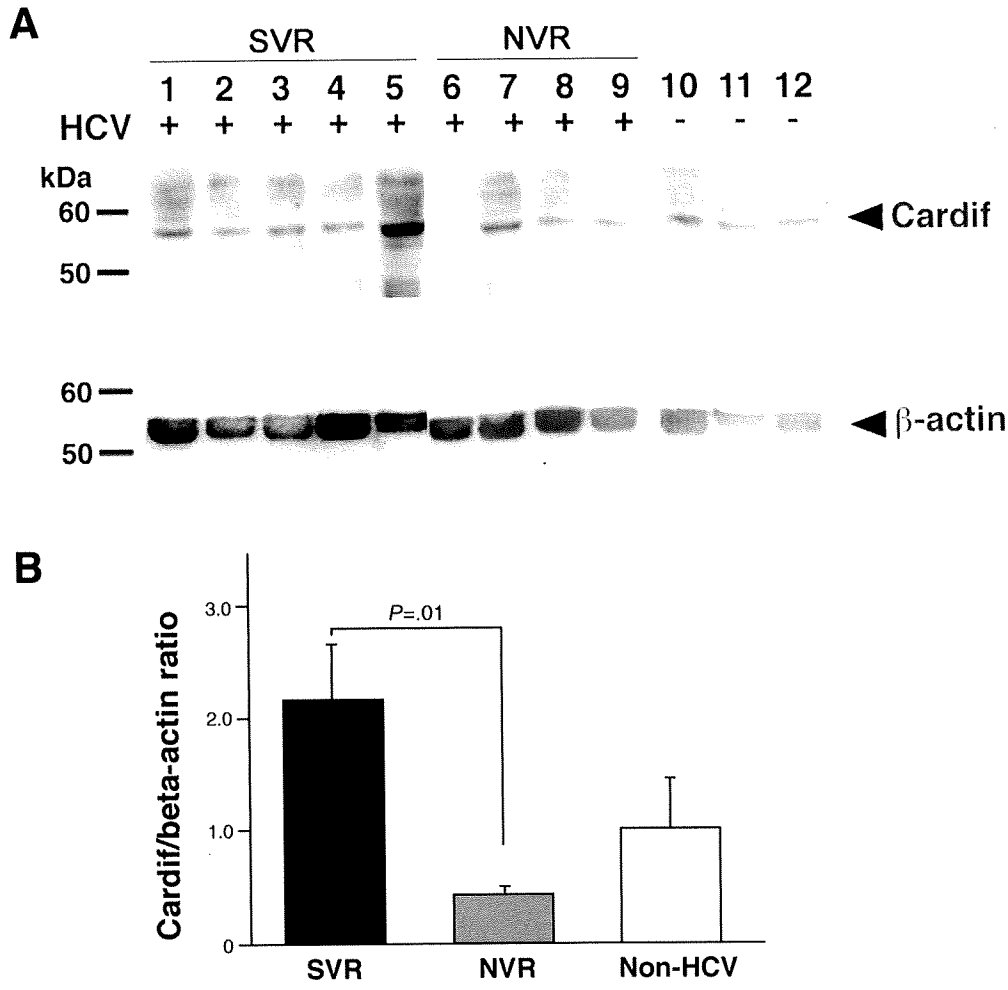

Figure 4. (*A*) Western blot analysis. Five lanes were SVR (*lanes 1–5*), 4 lanes were NVR (*lanes 6–9*), and 3 lanes were non-HCV control (*lanes 10–12*). Specific bands for Cardif and β-actin are indicated by *arrows*. (*B*) Expression level of Cardif protein normalized to β-actin in the liver biopsy specimens according to ultimate treatment response. *Error bars* indicate the standard error.

in these patients, suggesting that NVR patients may have adopted a different equilibrium in their immune response to the virus. In contrast to the expression of RIG-I and MDA5, Cardif mRNA, which was expressed in a relatively constitutive fashion, was significantly lower in NVR. Our ROC analysis highlights that lower expression of Cardif relative to that of RIG-I was one of the strongest predictors for NVR. Moreover, Western blot analysis further confirmed the down-regulation of Cardif in NVR patients, as demonstrated by its protein level. Because Cardif is one of the substantial target molecules of HCV evasion,[11,20] it is likely that Cardif expression is suppressed by HCV with resistant phenotype or is inadequate in NVR patients. Loo et al have demonstrated a Cardif cleavage product in 2 of 4 liver tissue samples of chronic HCV infection.[23] In our study, however, the Cardif cleavage product was not detected, presumably because the product could be unstable in vivo, resulting in rapid degradation. Although further studies are necessary to elucidate mechanisms of Cardif down-regulation, our findings of lower expression of Cardif in NVR suggested that the status of Cardif expression in the liver might have a significant effect on the ultimate outcome of antiviral treatment.

The antiviral effect brought by RIG-I/Cardif signaling is regulated by the coordination of negative and positive regulators. It has been shown that RNF125 functions as a negative regulator of RIG-I/Cardif signaling. RNF125 is an ubiquitin E3-ligase with activity against protein containing CARD domains, such as RIG-I, MDA5, and Cardif, and these ubiquitinated molecules undergo proteasomal degradation. In contrast, RNF125 do not have negative function against LGP2, a negative regulator of RIG-I signaling, because LGP2 lacks CARD domain. In contrast to RIG-I, RNF125 expression was rapidly suppressed by exogenous IFN; therefore, observed lower basal hepatic level of RNF125 in NVR could be explained by the suppressive effect of endogenous IFN, which may be up-regulated in NVR patients. Hence, RNF125 may constitute a negative regulatory circuit for IFN production and is responsible for responsiveness to PEG-IFN and ribavirin therapy.

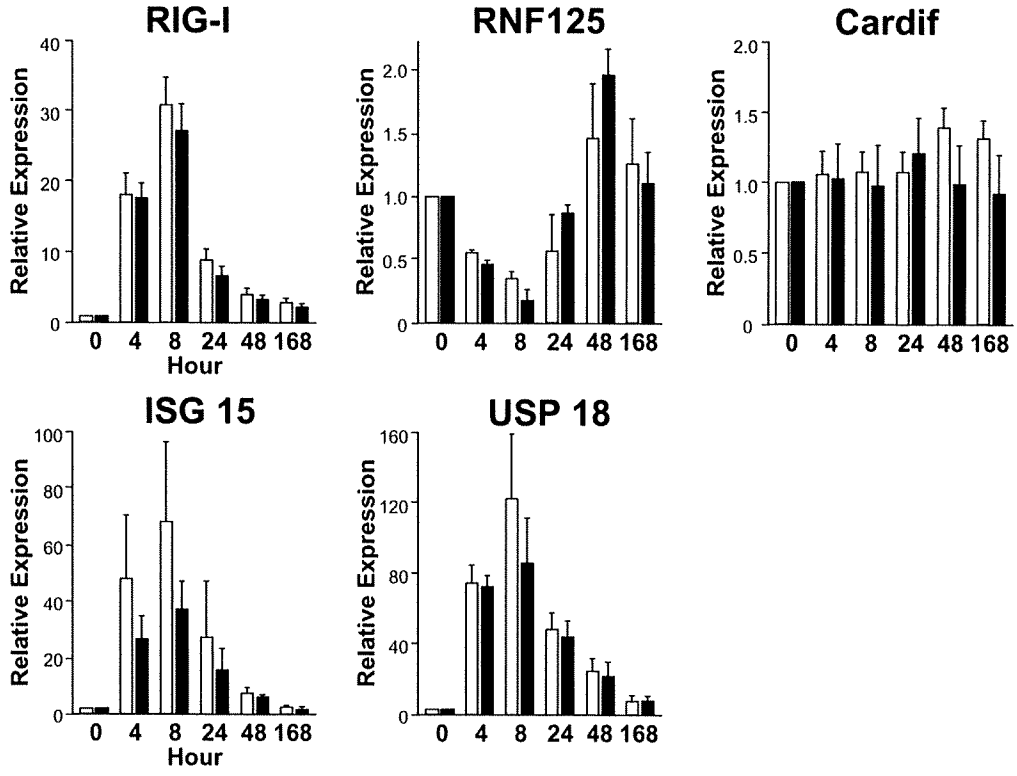

Figure 5. Transcriptional responses during PEG-IFN-α-2b and ribavirin therapy in PBMC (n = 14). *Open columns* indicate SVR (n = 7), and *solid columns* indicate NVR (n = 7). *Error bars* indicate the standard error. The *P* values determined by Mann–Whitney *U* test between 2 groups at 8 hours were as follows: RIG-I, *P* .3; RNF125, *P* .3; Cardif, *P* .7; ISG15, *P* .3; USP18, *P* .2.

It has been shown that RIG-I function is modified by ISG15 via ISGylation.[17] Consistent with our data, Chen et al identified 18 genes, including ISG15 and USP18, whose expression differed between responders and non-responders.[26] Interestingly, a recent study has shown that USP18 negatively regulates IFN signaling independently of its isopeptidase activity toward ISG15 by binding to the IFNAR2 receptor subunit and blocking the interaction between Janus kinase and the IFN receptor.[27] Moreover, the siRNA knockdown of USP18 in human cells has consistently been shown to potentiate the ability of IFN to inhibit HCV RNA replication.[28] Therefore, USP18 is suggested as a novel in vivo inhibitor of signal transduction pathways that are specifically triggered by type I IFN. Consistent with a role for USP18 in down-regulating the antiviral IFN response, we confirmed that up-regulation of USP18 was one of the factors predicting a lack of response to treatment with IFN.

The mechanism underlying the association of gene expression involving innate immunity with resistance to therapy is not well understood. Our human study with HCV patients treated by PEG-IFN and ribavirin highlights RIG-I/Cardif, RIG-I/RNF125, and ISG15/USP18, which is partly responsible for the clinical responsiveness to antiviral therapy. RIG-I signaling by viral pathogens may affect a wide variety of responses in not only innate but also acquired immunity. Our study is the first to demonstrate the potential relevance between molecules involving innate immunity and the clinical response to antiviral therapy.

In addition, sequential analysis of expression profile during PEG-IFN-α-2b and ribavirin treatment was also performed in this study. Lanford et al demonstrated transcriptional response to IFN-α in chimpanzee by genome microarray analysis, which included RIG-I, ISG15, and USP18.[29] An association of transcriptional response with early phase of virologic response has been also reported in PBMC or liver biopsy specimen.[30–32] We recently reported that the transcriptional double-stranded RNA-activated protein kinase response during treatment with PEG-IFN-α-2b and ribavirin was associated with the ultimate clinical response.[30] Similarly, the present study demonstrated a strong and rapid increase of RIG-I, ISG15, and USP18 mRNA in response to clinical PEG-IFN treatment especially in SVR patients, although few patients were available to achieve statistical significance between SVR and NVR. In marked contrast, transcriptional response of RNF125 exhibited a triphasic pattern. Rapid suppression seen in the first phase was presumably because of a negative regulatory effect of IFN. However, increase of RNF125 mRNA in the second phase, which tended to be grater in NVR, may be responsible for inhibiting RIG-I expression seen 8–48 hours after PEG-IFN-α-2b administration. Although limitations includ-

ing the use of PBMC and small sample size still deserve mention, the sequential expression profile during treatment may provide further valuable information regarding the prediction of the clinical response to the therapy and the mechanism of action of antiviral treatment.

In the present study, we have included patients with genotype 1b because it is imperative to designate a virologically homogeneous patient group to associate individual treatment responses with different gene expression profiles that direct innate immune responses. We have preliminarily studied genotype 2 patients and found that Cardif and RNF125 gene expression levels in NVR patients were significantly lower than those with SVR patients ($P = .03$ and $P = .04$, respectively) and that RIG-I/Cardif and RIG-I/RNF125 ratios were significantly higher in NVR patients ($P = .02$ and $P = .009$, respectively, see Supplementary Figure 2 online at www.gastrojournal.org). These findings suggest that the differences in gene expression profiles between SVR and NVR were almost identical to those demonstrated in patients with genotype 1b. However, the correlation between treatment responses in all the genotypes and the different status of innate immune responses needs to be explored. Further studies may be necessary to clarify this issue.

In conclusion, the results of the present study offer potentially important clinical implications for patients with chronic hepatitis C who are treated with PEG-IFN-α and ribavirin. Quantifying hepatic gene expression of the RIG-I/Cardif system, including its regulators before treatment, is useful in identifying patients who are at a higher risk for NVR. The data from these assays can provide valuable information that may influence the decision about the treatment strategy in each individual patient. Finally, this clinical human study demonstrates the potential relevance of the molecules involving innate immunity to the clinical response to therapy. Our data will help understand the pathogenesis of HCV resistance and development of new antiviral therapy targeted toward the innate immune system.

Supplementary Data

Note: To access the supplementary material accompanying this article, visit the online version of *Gastroenterology* at www.gastrojournal.org, and at doi: 10.1053/j.gastro.2008.02.019.

References

1. Kiyosawa K, Sodeyama T, Tanaka E, et al. Interrelationship of blood transfusion, non-A, non-B hepatitis and hepatocellular carcinoma: analysis by detection of antibody to hepatitis C virus. Hepatology 1990;12:671–675.
2. Manns MP, McHutchison JG, Gordon SC, et al. Peginterferon alfa-2b plus ribavirin compared with interferon alfa-2b plus ribavirin for initial treatment of chronic hepatitis C: a randomised trial. Lancet 2001;358:958–965.
3. Fried MW, Shiffman ML, Reddy KR, et al. Peginterferon alfa-2a plus ribavirin for chronic hepatitis C virus infection. N Engl J Med 2002;347:975–982.
4. Hadziyannis SJ, Sette HJ, Morgan TR, et al. PEGASYS International January 2006 American Gastroenterological Association 253 Study Group. Peginterferon-α-2a and ribavirin combination therapy in chronic hepatitis C: a randomized study of treatment duration and ribavirin dose. Ann Intern Med 2004;140:346–355.
5. Zeuzem S, Pawlotsky JM, Lukasiewicz E, et al. DITTO-HCV Study Group. International, multicenter, randomized, controlled study comparing dynamically individualized versus standard treatment in patients with chronic hepatitis C. J Hepatol 2005;43:250–257.
6. Berg T, von Wagner M, Nasser S, et al. Extended treatment duration for hepatitis C virus type 1: comparing 48 versus 72 weeks of peginterferon-alfa-2a plus ribavirin. Gastroenterology 2006;130:1086–1097.
7. Biron CA. Initial and innate responses to viral infections—pattern setting in immunity or disease. Curr Opin Microbiol 1999;2:374–381.
8. Gale M Jr, Foy EM. Evasion of intracellular host defence by hepatitis C virus. Nature 2005;436:939–945.
9. Yoneyama M, Kikuchi M, Natsukawa T, et al. The RNA helicase RIG-I has an essential function in double-stranded RNA-induced innate antiviral responses. Nat Immunol 2004;5:730–737.
10. Yoneyama M, Kikuchi M, Matsumoto K, et al. Shared and unique functions of the DExD/H-box helicases RIG-I, MDA5, and LGP2 in antiviral innate immunity. J Immunol 2005;175:2851–2858.
11. Meylan E, Curran J, Hofmann K, et al. Cardif is an adaptor protein in the RIG-I antiviral pathway and is targeted by hepatitis C virus. Nature 2005;437:1167–1172.
12. Kawai T, Takahashi K, Sato S, et al. IPS-1, an adaptor triggering RIG-I- and Mda5-mediated type I interferon induction. Nat Immunol 2005;6:981–988.
13. Seth RB, Sun L, Ea CK, et al. Identification and characterization of MAVS, a mitochondrial antiviral signaling protein that activates NF-κB and IRF 3. Cell 2005;122:669–682.
14. Xu LG, Wang YY, Han KJ, et al. VISA is an adapter protein required for virus-triggered IFN-β signaling. Mol Cell 2005;19:727–740.
15. Rothenfusser S, Goutagny N, DiPerna G, et al. The RNA helicase Lgp2 inhibits TLR-independent sensing of viral replication by retinoic acid-inducible gene-I. J Immunol 2005;175:5260–5268.
16. Arimoto K, Takahashi H, Hishiki T, et al. Negative regulation of the RIG-I signaling by the ubiquitin ligase RNF125. Proc Natl Acad Sci U S A 2007;104:7500–7505.
17. Zhao C, Denison C, Huibregtse JM, et al. Human ISG15 conjugation targets both IFN-induced and constitutively expressed proteins functioning in diverse cellular pathways. Proc Natl Acad Sci U S A 2005;102:10200–10205.
18. Schwer H, Liu LQ, Zhou L, et al. Cloning and characterization of a novel human ubiquitin-specific protease, a homologue of murine UBP43 (Usp18). Genomics 2000;65:44–52.
19. Malakhov MP, Malakhova OA, Kim KI, et al. UBP43 (USP18) specifically removes ISG15 from conjugated proteins. J Biol Chem 2002;277:9976–9981.
20. Li XD, Sun L, Seth RB, et al. Hepatitis C virus protease NS3/4A cleaves mitochondrial antiviral signaling protein off the mitochondria to evade innate immunity. Proc Natl Acad Sci U S A 2005;102:17717–17722.
21. Nakagawa M, Sakamoto N, Tanabe Y, et al. Suppression of hepatitis C virus replication by cyclosporin A is mediated by blockade of cyclophilins. Gastroenterology 2005;129:1031–1041.
22. Asahina Y, Izumi N, Uchihara M, et al. A potent antiviral effect on hepatitis C viral dynamics in serum and peripheral blood mononuclear cells during combination therapy with high-dose daily

interferon α plus ribavirin and intravenous twice-daily treatment with interferon β. Hepatology 2001;34:377–384.
23. Loo YM, Owen DM, Li K, et al. Viral and therapeutic control of IFN-β promoter stimulator 1 during hepatitis C virus infection. Proc Natl Acad Sci U S A 2006;103:6001–6006.
24. Dienstag JL, McHutchison JG. American Gastroenterological Association technical review on the management of hepatitis C. Gastroenterology 2006;130:231–264.
25. National Institutes of Health. National Institutes of Health Consensus Development Statement: management of hepatitis. Hepatology 2002;36(Suppl 1):S3–S20.
26. Chen L, Borozan I, Feld J, et al. Hepatic gene expression discriminates responders and nonresponders in treatment of chronic hepatitis C viral infection. Gastroenterology 2005;128:1437–1444.
27. Malakhova OA, Kim KI, Luo JK, et al. UBP43 is a novel regulator of interferon signaling independent of its ISG15 isopeptidase activity. EMBO J 2006;25:2358–2367.
28. Randall G, Chen L, Panis M, et al. Silencing of USP18 potentiates the antiviral activity of interferon against hepatitis C virus infection. Gastroenterology 2006;131:1584–1591.
29. Lanford RE, Guerra B, Lee H, et al. Genomic response to interferon-α in chimpanzees: implications of rapid down-regulation for hepatitis C kinetics. Hepatology 2006;43:961–972.
30. Asahina Y, Izumi N, Umeda N, et al. Pharmacokinetics and enhanced PKR response in patients with chronic hepatitis C treated with pegylated interferon α-2b and ribavirin. J Viral Hepat 2007;14:396–403.
31. Taylor MW, Tsukahara T, Brodsky L, et al. Changes in gene expression during pegylated interferon and ribavirin therapy of chronic hepatitis C virus distinguish responders from nonresponders to antiviral therapy. J Virol 2007;81:3391–3401.
32. Feld JJ, Nanda S, Huang Y, et al. Hepatic gene expression during treatment with peginterferon and ribavirin: identifying molecular pathways for treatment response. Hepatology 2007;46:1548–1563.

Received August 30, 2007. Accepted January 31, 2008.

Address requests for reprints to: Namiki Izumi, MD, PhD, Chief, Department of Gastroenterology and Hepatology, Musashino Red Cross Hospital, 1-26-1 Kyonan-cho, Musashino-shi, Tokyo 180-8610, Japan. e-mail: nizumi@musashino.jrc.or.jp; fax: (81) 422-32-9551.

Supported by grants from the Miyakawa Memorial Research Foundation; the Japanese Ministry of Education, Culture, Sports, Science and Technology; and the Japanese Ministry of Welfare, Health and Labor.

Financial disclosures: The authors who participated in this study have had no affiliation with the manufacturers of the drugs involved either in the past or in present and have not received funding from the manufacturers to conduct this research.

Targeting Lipid Metabolism in the Treatment of Hepatitis C Virus Infection

Fumitake Amemiya,[1,a] Shinya Maekawa,[1,a] Yoshie Itakura,[1] Asuka Kanayama,[1] Akira Matsui,[1] Shinichi Takano,[1] Tatsuya Yamaguchi,[1] Jun Itakura,[1] Takatoshi Kitamura,[1] Taisuke Inoue,[1] Minoru Sakamoto,[1] Kozue Yamauchi,[1] Shunichi Okada,[1] Atsuya Yamashita,[2] Naoya Sakamoto,[3] Masahiko Itoh,[2] and Nobuyuki Enomoto[1]

[1]First Department of Internal Medicine and [2]Department of Microbiology, Faculty of Medicine, University of Yamanashi, Yamanashi, and [3]Department of Gastroenterology and Hepatology, Tokyo Medical and Dental University, Tokyo, Japan

Recently, microdomains of organelle membranes rich in sphingomyelin and cholesterol (called "lipid rafts") have been considered to act as a scaffold for the hepatitis C virus (HCV) replication complex. Using the HCV cell culture system, we investigated the effect of myriocin, a sphingomyelin synthesis inhibitor, on HCV replication. We also investigated the combined effect of myriocin with interferon (IFN) and myriocin with simvastatin. Myriocin suppressed replication of both a genotype 1b subgenomic HCV replicon (Huh7/Rep-Feo) and genotype 2a infectious HCV (JFH-1 HCV) in a dose-dependent manner (for subgenomic HCV-1b, maximum of 79% at 1000 nmol/L; for genomic HCV-2a, maximum of 40% at 1000 nmol/L). Combination treatment with myriocin and IFN or myriocin and simvastatin attenuated HCV RNA replication synergistically in Huh7/Rep-Feo cells. Our data demonstrate that the sphingomyelin synthesis inhibitor strongly suppresses replication of both the subgenomic HCV-1b replicon and the JFH-1 strain of genotype 2a infectious HCV, indicating that lipid metabolism could be a novel target for HCV therapy.

Hepatitis C virus (HCV) is a major etiologic agent of liver diseases, affecting 170 million people worldwide [1]. Fifty-five percent to 85% of acute infections become persistent [2], and at least 20% of patients with chronic HCV infection progress to cirrhosis within 20 years [3]. With therapeutic advances, including the recent combination of pegylated interferon (IFN) plus ribavirin, half of patients can achieve a sustained virologic response [4]. However, the remaining half cannot clear the virus, demonstrating a strong need for HCV-specific therapies.

Positive-strand RNA viruses replicate intracellularly on certain membrane structures, including the endoplasmic reticulum [5], the Golgi apparatus [6], endosomes, and lysosomes [7]. During replication, RNA viruses form distinct replication complexes made of several membrane compartments and viral proteins [8]. In HCV, the membranous web (consisting of vesicles in a membranous matrix) has been described in the cellular matrix of HCV replicon–harboring cells [9, 10]. This membranous web is considered to be the HCV replication complex, consisting of viral and host proteins.

Recent studies suggest that the HCV replication complexes are formed on lipid rafts (which are detergent-insoluble microdomains of intracellular vesicular membranes rich in cholesterol and sphingolipid) [11–13]. It has been reported that viral nonstructural proteins and both positive- and negative-sense HCV RNAs were localized distinctively in a fraction of lipid rafts when subgenomic HCV replicon cells were subjected to membrane flotation analysis [12]. On the other hand, recent studies have demonstrated that agents related to lipid metabolism affect the replication of genotype 1 HCV. Leu et al. [14] reported that polyunsaturated fatty acids exerted strong anti-HCV activity on a subgenomic HCV-1b replicon. Moreover, 3-hydroxy-3-methylglutaryl coenzyme A (HMG-CoA) reductase inhibitors (statins), which prevent cholesterol synthesis, have been shown to suppress replication of ge-

Received 29 May 2007; accepted 24 September 2007; electronically published 23 January 2008.

Potential conflicts of interest: none reported.

Financial support: Japanese Ministry of Education, Culture, Sports, Science, and Technology (scientific research grant 17390216).

[a] F.A. and S.M. contributed equally to this work.

Reprints or correspondence: Dr. Shinya Maekawa, First Department of Internal Medicine, Faculty of Medicine, University of Yamanashi, 1110, Shimokato, Chuo, Yamanashi 409–3898, Japan (maekawa@yamanashi.ac.jp).

The Journal of Infectious Diseases 2008; 197:361–70

© 2008 by the Infectious Diseases Society of America. All rights reserved.

0022-1899/2008/19703-0007$15.00

DOI: 10.1086/525287

nomic and subgenomic HCV-1b replicons [15, 16]. Even though the precise mechanism has not been defined, these agents may attenuate HCV replication through the destruction of lipid rafts, according to their pharmacological actions. If this is the mechanism, sphingomyelin, the remaining and essential component of lipid rafts, might play a role in HCV replication. With this in view, recent studies have demonstrated that a sphingomyelin synthesis inhibitor attenuated the replication of a subgenomic HCV-1b replicon in cultured cells [17] and the replication of genomic HCV-1 in a chimeric mouse model [18]. However, investigation of anti-HCV activity in these agents has been limited to genotype 1 HCV, and the combined effect of these agents has not been determined. If they do not target the HCV structure itself but exert their antiviral activity through destruction of the host's lipid raft, it would be plausible to speculate that they might be effective irrespective of the viral isolate, and the combined effect of these agents might be additive or synergistic.

In the present study, we investigated the role played by the sphingomyelin synthesis pathway and the mevalonate pathway in HCV replication, using a subgenomic HCV-1b replicon and the particle-producing cell culture HCV 2a model of JFH-1 HCV [19].

MATERIALS AND METHODS

Cell culture and HCV replicon. The human hepatoma cell lines Huh7 and Huh7.5.1 [20] were maintained in Dulbecco's modified Eagle's medium (Sigma) supplemented with 10% fetal calf serum at 37°C in 5% CO_2. The subgenomic HCV replicon used was derived from Rep-Feo (genotype 1b) [21, 22], and a full-length genomic HCV RNA was derived from genotype 2a JFH-1 HCV [19]. Subgenomic or genomic HCV RNA was synthesized from replicon cDNA–harboring plasmids (pRep-Feo and pJFH-1) by means of T7 polymerase (RiboMax Large Scale RNA Production System; Promega) and transfected into these cells. For the subgenomic replicon, cell lines stably expressing the replicon were established (Huh7/Rep-Feo) in the presence of 500 μg/mL G418.

Reporter plasmids and luciferase assay. pISRE-TA-Rluc expressing the *Renilla* luciferase reporter gene under control of the IFN-stimulated response element (ISRE) was constructed by replacing the firefly luciferase gene with the *Renilla* luciferase gene of pISRE-TA-Luc, purchased from Invitrogen. Luciferase activity was quantified using the Bright-Glo or Dual-Luciferase assay system (both from Promega) and a luminometer (AB-2250; ATTO). Assays were performed in triplicate, and the results were expressed as mean ± SD percentages of the control values. QuantiLum recombinant luciferase (Promega) was used as the positive control for the analysis.

Reagents. The reagents used included myriocin (Biomol), IFN-α 2b (Santa Cruz Biotechnology), phytosphingosine hydrochloride (Sigma), 2-hydroxypropyl-β-cyclodextrin (2-HP-β-CyD; Sigma), and simvastatin (Cosmobio).

Northern blotting. Total cellular RNA was extracted from cells by means of Isogen (Wako). The RNA was separated by denaturing agarose-formaldehyde gel electrophoresis and transferred to a membrane from a NorthernMax kit (Ambion). The membrane was hybridized with a digoxigenin-labeled probe that was specific for the nonstructural replicon sequence. The signals were detected in a chemiluminescence reaction by using a digoxigenin detection kit (Roche) and were visualized by using an LAS-1000 imaging system (Fuji Film).

Western blotting. Ten micrograms of total cell lysate was separated using NuPAGE 4%–12% Bis-Tris gel (Invitrogen) and was blotted onto an Immobilon polyvinylidene difluoride membrane (Roche). The membrane was incubated with an anti-core monoclonal antibody (MAb; Affinity Bioreagents), an anti-NS3 MAb (Virogen), an anti-NS5A MAb (gift from Burckstummer, Robert Koch Institute), or a anti–β-catenin MAb (Sigma). Detection was done in a chemiluminescence reaction (ECL; Amersham).

Dimethylthiazol carboxymethoxyphenyl sulfophenyl tetrazolium (MTS) assays. To evaluate cytotoxicity, MTS assays were performed using a CellTiter 96 Aqueous One Solution Cell Proliferation Assay (Promega), in accordance with the manufacturer's instructions.

Thin-layer chromatography (TLC). The lipid fraction of cells treated with myriocin was extracted using the method of Bligh and Dyer [23], and total lipids from the cells treated with myriocin were extracted with 3 mL of chloroform. The extracts were spotted onto silica gel TLC plates (Merck) and were chromatographed with chloroform-methanol-water (65:25:4 [vol/vol/vol]). The plate was visualized with a molybdenum spray.

Real-time reverse-transcription polymerase chain reaction (RT-PCR). TaqMan RT-PCR targeting the 5' untranslated region was used for the quantitation of intracellular genomic JFH-1 HCV RNA. The sequences of the sense and antisense primers and the TaqMan probe were 5'-TGCGGAACCGGTGAGTACA-3', 5'-CTTAAGGTTTAGGATTCGTGCTCAT-3', and 5'-(FAM)CAC-CCTATCAGGCAGTACCACAAGGCC(TAMRA)-3', respectively. The method has been described elsewhere [24].

Short interfering RNA (siRNA) analysis. The sequence encoding the LCB1 subunit of serine palmitoyltransferase (SPT) was selected as the target for siRNA (sense, 5'-AACAA-CAUCGUUUCAGGUCCUTT-3'; antisense, 5'-AGGGCCUG-AAACGAUGUUGTT-3'). siRNA targeting enhanced green fluorescent protein (GFP) was used as the negative control (sense, 5'-CUUACGCUGAGUACUUCGATT-3'; antisense, 5'-UCG-AAGUACUCAGCGUAATT-3'). (Underlined letters indicate deoxyribonucleotides.)

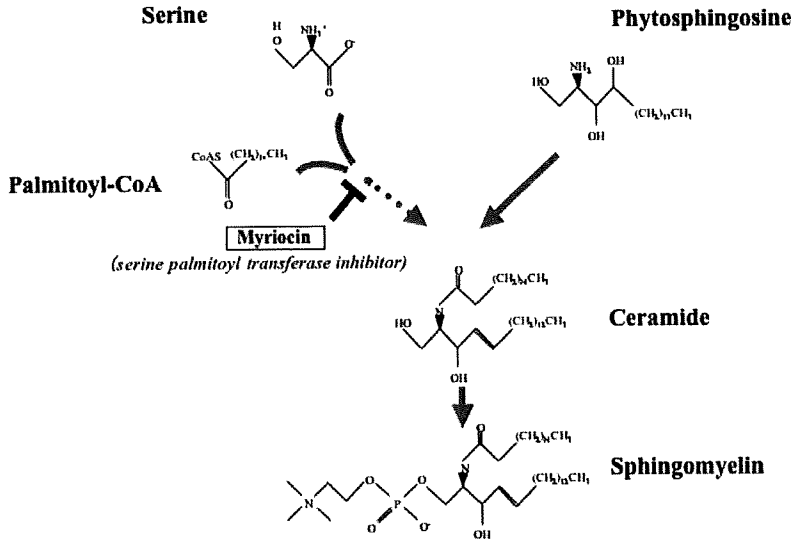

Figure 1. The sphingomyelin synthesis pathway. Serine palmitoyltransferase catalyzes the first committed step of sphingomyelin biosynthesis from serine and palmitoyl-coenzyme A (CoA). Myriocin inhibits the catalyzing activity of serine palmitoyltransferase. Phytosphingosine is known to work as a precursor of ceramide in both mammalian and fungal cells.

Statistical analyses. Statistical analyses were performed using Student's *t* test; statistically significant differences were defined as those for which $P < .05$.

RESULTS

Specific suppression of the replication of a subgenomic HCV-1b replicon by an inhibitor of sphingomyelin synthesis. To clarify the role played by the sphingomyelin synthesis pathway in HCV replication, we added myriocin, a specific inhibitor of SPT that catalyzes the first committed step of sphingomyelin biosynthesis (figure 1), to the medium of Huh7/Rep-Feo cells. The luciferase activity, reflecting replication of the subgenomic HCV-1b replicon, dropped to 37% and 21% of the control at myriocin concentrations of 100 and 1000 nmol/L, respectively (figure 2*A*, *upper panel*), but myriocin did not cause toxicity to the cultured cells (figure 2*A*, *lower panel*). The result indicates that the decrease in HCV replication is due to a specific suppressive effect of myriocin and not to the cytotoxicity of myriocin. Northern hybridization analysis also demonstrated a substantial reduction of the subgenomic HCV replicon RNA in Huh7/Rep-Feo cells treated with myriocin in a dose-dependent manner (figure 2*B*). Similarly, Western blot analysis demonstrated a decrease in HCV NS5A after treatment with myriocin (figure 2*C*).

No enhancement of ISRE promoter activity after myriocin treatment. To determine whether the effect of myriocin in suppressing the subgenomic HCV replicon was associated with the activation of IFN-stimulated genes, the ISRE–*Renilla* luciferase plasmid was transfected into Huh7/Rep-Feo cells, and these cells were cultured with various concentrations of myriocin. As a positive control for the enhancement of ISRE reporter activity, the ISRE–*Renilla* luciferase–transfected cells were cultured with IFN. Myriocin had no significant effect on ISRE promoter activity, whereas IFN significantly up-regulated ISRE activity (figure 2*D*, *upper panel*). In contrast, firefly luciferase activity in the Huh7/Rep-Feo cells, reflecting HCV replication, was inhibited by both IFN and myriocin in a dose-dependent manner (figure 2*D*, *lower panel*). These results demonstrate that the action of myriocin on HCV replication is independent of the IFN pathway.

Decrease in the sphingomyelin content of Huh7 cells after myriocin treatment. To clarify whether myriocin really inhibits the biosynthesis of sphingomyelin in Huh7 cells, we treated Huh7 cells with 100 nmol/L myriocin and analyzed the change in the cellular phospholipid composition by TLC. As demonstrated in figure 2*E*, the cellular sphingomyelin content decreased after myriocin treatment, but no significant change was observed in other cellular phospholipids.

Restoration of HCV replication by addition of phytosphingosine. To confirm that suppression of HCV RNA replication was due to depletion of sphingomyelin, we incubated replicon cells with phytosphingosine, a precursor of ceramide in mammalian and fungal cells, in the presence of myriocin. Treatment with phytosphingosine restored HCV replication in a dose-dependent manner (figure 2*F*, *upper panel*). On the other hand, phytosphingosine by itself did not have any effect on HCV replication (figure 2*F*, *lower panel*). This result indicates that inhibition of HCV replication was the direct result of depletion of sphingomyelin.

Suppression of HCV replication by knocking down SPT with siRNA. Next, we determined whether inhibition of SPT expression suppresses HCV replication by knocking down SPT with siRNA. As demonstrated in the upper panel of